An investigation of how intracratonic rifting is "seeded": case study of the Late Devonian Dniepr-Donets Basin rift within the East European Craton

by

Randell Stephenson[1], Tamara Yegorova[2], Sergiy Stovba[2]

1 - School of Geosciences, University of Aberdeen, King's College, Aberdeen AB24 3UE, Scotland

2 - Institute of Geophysics, National Academy of Sciences of Ukraine, Kyiv, Ukraine

Abstract

This paper analyses the role of pre-existing Precambrian structures for the localisation of the intracratonic rifts from a case study of the Dniepr-Donets Basin (DDB) in Ukraine. The DDB was formed as a result of Late Palaeozoic rifting in the Archaean-Paleoproterozoic Sarmatian segment of the East European craton (EEC). It separates the Ukrainian Shield (UkS) to its southwest from the Voronezh Massif (VM) to its northeast. The Donbas Foldbelt (DF) constitutes the tectonically inverted part of the DDB in its southeastern extent and has been imaged by coincident wide-angle reflection and refraction seismic as well as deep near-vertical reflection seismic profiles (project "DOBRE"). It is almost completely filled with a highly indurated succession of upper Palaeozoic sediments and metasediments, up to some 20 km in thickness, now exposed at the surface. Here, a crustal and upper mantle structural-compositional model that is tightly constrained by the seismic data and gravity anomalies along the profile is used to search for Precambrian pre-rift crustal features that could have played a role in localising Late Palaeozoic rifting. The results suggest that there may be a different tectonic history for Sarmatian crystalline crust on either side of the DF. Density isolines in the AM crust are shallower than corresponding ones of equal value in the VM crust and, accordingly, the mean density of the crust of the AM is higher. This effect, calibrated on the DOBRE profile, is expressed along the margins of the entire DDB with a higher background level of the gravity field seen generally for the UkS than for the VM. The associated gravity gradient coinciding with the location of Palaeozoic rifting means that there is a perturbation to the horizontal deviatoric stress in this position that likely predates rifting. Further, a well-constrained upper crustal low-density granitic body beneath the northeastern flank of the DF produces a significant negative gravity anomaly superimposed upon the background gravity gradient. This adds a significant additional extensional component to the ambient deviatoric stress field. It cannot be concluded with certainty that either of these crustal features was necessary or sufficient for "seeding" Late Palaeozoic rifting but modern passive seismology surveys across the DDB as well as new bedrock geological studies would help test such a hypothesis.

Keywords: intracratonic rifting, inheritance, deep seismic profiling, gravity modelling, crustal structure, East European Craton, Sarmatia, Donbas Foldbelt, Dniepr-Donets Basin, Ukraine

1. Introduction

The Dniepr-Donets Basin (DDB) formed in the Late Palaeozoic as a narrow rift basin within the Archaean-Palaeoproterozoic crust of the East European Craton (EEC), as seen in Figure 1 (e.g., Chirvinskaya and Sollogub, 1980). Active rifting occurred in the Late Devonian after which post-rift thermal subsidence continued, though interrupted or modified by tectonic events in the Carboniferous, the Late Triassic and, especially, the Late Cretaceous-Paleogene when rift inversion and compressional shortening occurred (e.g., Stephenson et al., 2006). The DDB rift (and its northwestern prolongation, the Pripyat Trough) obliquely cross-cuts the regional structural trends mapped in the underlying crystalline basement and correlated across the rift (Shchipansky and Bogdanova, 1996), which is part of the Sarmatian segment of the EEC as defined by Bogdanova (1993) and Gorbatschev and Bogdanova (1993).

Continental rifts are among the most-studied crustal-scale geological features in all of tectonics and geodynamics and probably have been the object of more modelling studies – analogue and numerical – than any other feature of the Earth's continental crust of similar scale. They form when extensional tectonic stresses exceed the strength of crustal/lithospheric materials so that permanent deformation is inflicted upon the lithosphere, which can be described as "stretching" that produces thinning of the lithosphere. The structural response to the thinning process is basically one of isostasy: thinned crust (and consequent shallower upper mantle) is compensated by sediment, water and air in the rift basin. Thermal relaxation of the thinned, heated-up mantle lithosphere then produces longer term (thermal) subsidence. Rifts form in a multitude of tectonic settings, in lithosphere that is initially cold and strong (such as the DDB rift) or initially warm and weak and their structural expression typically reflects ambient circumstances of formation such as these (e.g., Buck, 1991; Stephenson, 1996).

But why do rifts form where they do? Obviously there needs to be a generation of extensional deviatoric stresses that are large enough to overcome the intrinsic strength of the lithosphere and effect the extensional strain (rifting) but what are the processes causing the traumatic stress? In some tectonic settings where rifting occurs these questions are fairly easy to answer, such as rifting in back-arc settings. Processes related to subduction – like the negative buoyancy effects of a cold, subducting lithosphere slab (e.g., Uyeda and Kanamori, 1979; Schellart, 2009; Yamasaki and Stephenson, 2011) – produce optimally orientated tension in the back-arc upper lithosphere, lithosphere which, in turn, has also been conveniently weakened by subduction-related thermal and metasomatic processes (e.g., Currie and

Hyndman, 2006; Currie et al., 2008). But what about rifts formed in otherwise stable, cold and rheologically strong intracratonic environments, such as the DDB rift? One thing is clear from the vast published literature on the subject and that is that heterogeneity and reactivation of inherited structures is a fundamental of intraplate rifting. Indeed, numerical models of the dynamics of rifting can never succeed unless some kind of lateral heterogeneity is "seeded" into the model as an initial condition in order to allow extensional strain to localise and for rifts to develop (e.g., Huismans and Beaumont, 2007).

This is the point of departure of the present paper, which is a consideration of why the DDB rift formed where it did. A tightly constrained density model of mass distribution within the crust and upper mantle of the most intensely rifted Donbas Foldbelt segment (DF; cf. Fig. 1) of the DDB (based on present-day sediment thickness and basement depth) is presented along a profile (called "DOBRE") that has been imaged by modern, coincident deep near vertical and wide-angle seismic reflection and refraction profiles acquired as part of the European Science Foundation EUROPROBE programme in the late 1990s and early 2000s (cf. Stephenson et al., 2006 and references therein). The role played by the pre-existing crustal architecture as inferred from the density model combined with the considerable existing knowledge bank on the basement geology of the area is then discussed in the context of the processes that controlled the formation of the DDB and DF, as well as modelling and field studies generally of how rifting is localised in intracontinental lithosphere.

2. Geology

2.1 Precambrian basement

The Late Palaeozoic DDB rift cuts across the Archaean-Palaeoproterozoic crust of Sarmatia, the southernmost of three major segments forming the EEC (e.g., Bogdanova et al., 2016); the area north(east) of the DDB is called the Voronezh Massif (VM; Fig. 1), mostly overlain by a thin layer (generally less than 250 m thick) of Palaeozoic and Mesozoic sediments, whereas Sarmatian crust to the south(west) of the DDB is largely exposed as the Ukrainian Shield (UkS; Fig. 1). The UkS and VM together form a large basement uplift with a diameter of about 1000 km (Stephenson et al., 1993), within which the DDB rift formed. The crust of Sarmatia has traditionally been mapped in terms of regional "blocks" or litho-tectonic basement complexes (domains) separated by nearly north-south orientated sutures or "interblock zones" of Proterozoic age. Several of these can be correlated across the

Palaeozoic DDB rift zone from the UkS to the VM (e.g., Shchipansky and Bogdanova, 1996), as seen in Figure 1.

The crystalline basement of the southern part of the VM and north of the UkS (i.e., the northern and southern shoulders of the DDB, respectively), is buried beneath the broader Late Palaeozoic and younger post-rift sedimentary cover of the rift itself, in which areas the principal source of information on the basement geology is from subsurface samples obtained from drilling and, in a few cases, from industrial mines.

Figure 2 is a simplified, larger scale, basement map of the area of DOBRE, including contours indicating the thickness of the rift and rift shoulder sedimentary successions. The oldest rocks of the study area are found in the northern part of the Azov Massif (AM), which is the salient of the UkS adjacent to the DF where it is crossed by the DOBRE profile and are represented by Archaean mafic granulites and by mafic and ultramafic magmatic rocks (Zaritskii, 1992). Archaean granitoids are also present in the AM, expressed as domal plagio-granites throughout the area. The rocks of the AM generally display a higher grade of metamorphism than those of the VM to the north and northeast of the DF, where granitic and migmatitic rocks of reported Early Proterozoic age are widely distributed (Zaritskii, 1992). A suite of Paleoproterozoic alkaline-(ultra)mafic and alkaline intrusions occurs in the western part of the AM, which is also characterised by an abundance of dykes, typically alkaline in composition. In respect of the crust-mantle system of the AM, Gordienko and Usenko (2003), based on a study of mantle xenoliths, reported that the upper mantle of the AM has an anomalous composition, strongly depleted and metasomatised, in comparison to other domains of the UkS. Additional lithological details of basement rocks mapped in Figure 2 and their geophysical properties are listed in Table 1.

2.2 Late Palaeozoic formation and younger tectonic evolution of the DDB-DF

Traditional and modern views of the geology of the DDB rift basin (and DF) have been presented in numerous recent papers (cf. Stephenson et al., 2006, and abundant references therein, including the key reference work of Chirvinskaya and Sollogub, 1980) and a detailed repetition of this is not warranted here. A long-held view that the Late Palaeozoic rift formed above and reactivated an earlier Neoproterozoic-aged rift (e.g., Chekunov et al., 1992) was not substantiated by comprehensive subsurface mapping founded upon regional seismic reflection surveying (Stovba et al., 1996). Suffice further to say that the basin is characterised by a well-developed Late Devonian syn-rift sedimentary succession and a thick, mainly Carboniferous, post-rift succession. The total sedimentary package thickens from the

northwest to the southeast, reaching its maximum of some 20 km in the vicinity of the DF (Fig. 2). The termination of the DDB to the southeast is unclear because of tectonic overprinting from the Permo-Triassic (and perhaps as early as the Late Carboniferous) through the Cenozoic related to active convergence/transpressive processes on the nearby southern margin of Eurasia facing the complex of oceanic domains between Laurasia (Baltica) and Gondwana. It is likely that the DDB rift itself was subsumed into a complex system of structures and basins (including the Peri-Caspian Basin) on and beyond the late Palaeozoic margin of the EEC (e.g., Zonenshain et al., 1990; Saintot et al., 2006; cf. Barrier et al., 2018).

DDB rifting was accompanied by major magmatic activity in the Late Devonian (Wilson and Lyashkevich, 1996). Volcanic rocks of this age occur on the margins of the basin and are found in cap rocks of salt diapirs along the main axial inversion structure of the southeastern DDB (Garkalenko et al., 1971). The geochemical signature of rift-related magma (Wilson and Lyashkevich, 1996) plus the sheer volume of magma suggests that the origin of the DDB may have been mantle plume/hotspot related (e.g., Gavrish, 1989; Chekunov, 1994; Kusznir et al., 1996; Wilson and Lyashkevich, 1996). Subsidence modelling studies variously suggest that thinning of the mantle lithosphere during rifting was greater than crustal thinning (e.g., van Wees et al., 1996; Starostenko et al., 1999; Poplavskii et al., 2001), an effect that intensifies towards the DF in the southeast, and this is indirect evidence of a role for “active” rifting involving thermal processes in the mantle (e.g., Saintot et al., 2006; Stephenson et al., 2006).

A Permian unconformity is evident throughout much of the DDB, as it is throughout much of the remainder of the East European Platform (e.g., Mitrovica et al., 1996). Especially on the southern margin of the DDB, this unconformity shows angular discordance with underlying Carboniferous and earliest Permian strata. Much of the Upper Carboniferous and younger basin succession has been eroded in the DF, which also displays mild folding, thrusting, and reverse faulting (e.g., Stovba and Stephenson, 1999; Saintot et al., 2003ab). Thus, rocks exposed at the surface in the DF are mainly Carboniferous and, having been previously rather deeply buried, are highly indurated (e.g., Pogrebnov et al., 1985; cf. Popov, 1963; 1965ab).

Low temperature geochronology on the crystalline rocks of the AM adjacent to the DF suggests that the crystalline basement in this area reached its peak burial temperature in the Permo-Carboniferous but had cooled to near-surface temperatures during the Triassic with no observable thermal events thereafter (Danišík et al., 2008). These authors inferred that several kilometres of Devonian and Carboniferous strata were removed by the Triassic, which

compares to some 5-8 km based on correlation of absent sedimentary strata by Stovba and Stephenson (1999). There is also minor magmatism of Early Permian age reported by Alexandre et al. (2004) within basement rocks on the AM contiguous to the DF, also linked to the inferred uplift at this time.

Detailed studies of salt tectonics within the DDB document that the latest Carboniferous-Early Permian was a time of active halokinesis in a transtensional setting (Stovba and Stephenson, 1999; 2003) and that, accordingly, Early Permian uplift affecting the southern margins of the DDB and DF took place in a transtensional tectonic regime. The mechanism driving the stress regime and uplift at this time was likely related to thermo-mechanical processes at the southern boundary of the European plate, some 500 km to the south (Stampfli et al., 2013), such as changes in obliquity of plate convergence and possible detachment of partially subducted lithosphere (e.g., Saintot et al., 2006; cf. Muttoni et al, 2003; Meijers et al., 2010).

Basin inversion (compressional shortening) of the Late Palaeozoic DDB occurred mainly in the Late Cretaceous. (Saintot et al., 2003ab), Mesozoic sedimentary strata bordering the DF are unconformable, and show an erosional contact, with the underlying Carboniferous rocks indicating that some uplift occurred at this time and that the Carboniferous rocks of the DF, initially exhumed in the Permian, were likely re-exposed (Stovba et al., 1996; Kabyshev et al., 1998). There is also some evidence for compressional deformation during the Late Triassic (Stovba and Stephenson, 1999; Saintot et al., 2003ab), which is contemporaneous with significant Tethyan belt compressional tectonism on the nearby Karpinsky Swell (Sobornov, 1995), which, geographically speaking, represents the eastern prolongation of the DF (Fig. 1 inset). The culmination of Late Cretaceous basin inversion in the DDB and, ultimately, the formation of the DF, seems likely to be related to the contemporaneous onset of the Eo-Alpine orogenic phase in north-central Europe Ziegler (1990; cf. Stephenson et al., 2020).

3. Gravity field of the DDB and DF area

The structural and compositional model of the crust of the DDB, tightly constrained by regional seismic and rock lithology observations, is derived from gravity data. Figure 3 shows the regional Bouguer gravity field along the entire length of the rift basin and in more detail for the DF segment, in the top (a) and bottom (b) panels respectively.

The Dniepr segment of the DDB is characterised by positive gravity anomalies (values up to 40 mGal; Fig. 3a) along the rift axis, which is considered to be caused by the intrusion of what Starostenko et al. (1990) called an "axial dyke" of mafic rocks during Late Palaeozoic rifting. Further to the northwest, near the transition to the Pripyat Trough, Bouguer anomalies (values > 90 mGal) are among the highest of the whole East European Platform (Yegorova et al., 1995) and coincide with the occurrence of significant volumes of Late Devonian, rift-related, volcanics and intrusive rocks (e.g., Wilson and Lyashkevich, 1996). The Pripyat Trough itself is characterised by low gravity anomalies (values as low as -60 mGal) associated exclusively with the Palaeozoic and younger sedimentary succession (Yegorova et al., 2004a). Southeast from the Dniepr segment as far as the DF, where the thickness of the Devonian and younger sedimentary strata doubles, the gravity field pattern is dominated by an irregular gradient across which values to the north decrease northward towards the Voronezh Massif (VM).

The DF is characterised by a positive Bouguer anomaly with a maximum value of more than 40 mGal (Fig. 3b). A significant gravity low of similar amplitude lies on the northern flank of the DF and adjacent VM. Bouguer gravity values north and northeast of the gravity low are generally positive. Higher Bouguer anomalies (values > 20 mGal) are distinguished south of the DF in the vicinity of the Asov Massif and its eastern prolongation, which is known as the Rostov Uplift and is covered by a thin veneer of Mesozoic-Cenozoic sediments. The southwesternmost part of the DOBRE profile traverses a gravity high with values up to 40-50 mGal. These have been related to dense and highly metamorphosed Archaean rocks within the Azov Massif, including granulites (Golizdra and Akhmetshina, 1973), which are seen in the basement map presented in Figure 2.

A 3D gravity analysis carried out in the region of the DF (Yegorova et al., 1999; 2004b) revealed a distinct positive residual anomaly (contribution of sedimentary layers removed) along the axis of the rift basin, from the Dniepr-DF transition through the DF, and extending further to the southeast along the southern margin of the EEC. This was interpreted to be caused predominantly by high-density rocks in the crystalline crust, interpreted to be mafic and ultramafic rocks intruded into the crust during Late Palaeozoic rifting (Yegorova et al., 1999), similar to the "axial dyke" inferred by Starostenko et al. (1990) to the northwest.

4. Seismic and lithological constraints

4.1 Deep seismic refraction and reflection

The most important observations for constraining mass distribution in the crust and upper mantle from gravity modelling across the Donbas Foldbelt (DF) are the DOBRE deep seismic wide-angle reflection and refraction (WARR) and near-vertical reflection profiles. The former, 360 km long and acquired in 1999, provided a well resolved basin/crust/upper mantle P-wave velocity model across the DF and its margins (DOBREfraction'99 Working Group, 2003). This was augmented by deep near-vertical seismic reflection profiling, called DOBREflection in 1999 and 2000. Information about the DOBREflection acquisition and processing parameters can be found in Maystrenko et al. (2003) and Stovba et al. (2005). Figure 4a shows one WARR velocity model published by the DOBREfraction'99 Working Group (2003) and a skeletonised interpretation of the full DOBREflection deep seismic profile (km 70-330 in Fig. 4b) superimposed, in two-way travel-time (TWT), on a time-converted version of the former (km 0-360 in Fig. 4). This is a concise way to see both dataset interpretations. Any depths mentioned in the following paragraphs refer to those seen in the velocity model (Figure 4a), which is one of three very similar versions published as final products (DOBREfraction'99 Working Group, 2003), with very slight differences in detail not relevant to the descriptions below. The WARR data were of sufficient quality that S-wave phases were also recorded throughout much of the model space, allowing the ratio of P-wave and S-wave velocities (V_p/V_s) to be estimated in the main crystalline crustal domains and these are also indicated in Figure 4a.

Crystalline crust lies at the surface towards the southern end of the profile, in accordance with the exposed geology (cf. Fig. 2; Azov Massif, part of the UkS). Towards the northeast, on the southern part of the Voronezh Massif (cf. Fig. 2), it is overlain by a thin sedimentary succession along the extent of the seismic profile, its limited thickness confirmed by numerous boreholes (e.g., Maystrenko et al., 2003). Elsewhere, the general architecture of the sedimentary basin as seen in the reflection seismic image (Fig. 4b) is, as expected, a rift basin with pre-, syn- and post-rift successions (cf. Stephenson et al., 2006). It is generally compatible with the velocity model (Fig. 4a) taking into account the reduced resolving power of the refraction data. The boundary of the sedimentary succession and the top of underlying crystalline crust is indicated by the base of a parallel set of high impedance reflectors, marking the top and bottom of a thin, pre-rift (middle Devonian) platformal carbonate succession recognised in seismic profiles throughout the DDB (Stovba et al., 1996). This pair of reflectors is visible in Figure 4b (brown colour), disrupted by faults, between ~km 140-220 at 5-8 s TWT. Accordingly, the sedimentary package seen in Figure 4 comprises an asymmetric basin up to about 23 km depth. Several velocity layers are resolved within the

DF, shown in both Figure 4a and Figure 4b but with different colours for technical reasons. These do not precisely match the internal architecture of the basin as resolved by the reflection data; reflecting horizons within the sedimentary succession are shown as discrete coloured lines in Figure 4b. The lowest velocities (<3 km/s) occur in a near-surface layer on the northern border of the DF, where Cretaceous and, in places, younger sediments occur at the surface. The highly indurated Late Devonian and Carboniferous strata, which comprise the bulk of the sedimentary succession, display very high velocities for sedimentary rocks (> 5 km/s), compatible with observations of these strata in outcrop (Golizdra and Popovich, 1999; cf. Table 2). Refer to the Figure 4 caption for additional velocity information.

The DOBRE deep seismic reflection profile revealed intrabasinal structure indicating that Late Cretaceous shortening (inversion) of the rift took place in the form of a crustal-scale "pop-up" (Maystrenko et al., 2003), indicated by the red fault lines on Figure 4b. Its main component is an imbricate thrust zone, also evident in the exposed geology and confirmed by a 4500 m borehole, that disrupts the surface of the DF in the range km 215-230. The same thrust zone is interpreted to be responsible for the duplication of the basement marker horizons in the range ~km 180-190 as well as duplication of the Moho (see below) at km 100-110, thus cutting through the entire crust. A palinspastic reconstruction indicated that the tectonic shortening taking place at this time was about 12 km in total, mainly accommodated on the main thrust and its complementary back thrust) but with some shortening was taken up by intrabasinal folding as seen in the sedimentary succession of Figure 4b (Maystrenko et al., 2003). Stephenson et al. (2009) demonstrated that geometry of the "pop-up" structure and its localisation within the rift basin was strongly facilitated by the rheological effects of the thick succession of lower thermal conductivity sediments sitting within higher thermal conductivity crystalline crust.

The Moho in the reflection seismic image appears as a 1-2 s wide zone of strong reflectivity that is absent or disrupted to the northeast (~km 260-310). The refraction Moho (labelled M in Fig. 4b) corresponds with the base of this reflective zone and is approximately flat at a depth of about 40 km along the entire profile (the undulations seen in Figure 4 being slightly exaggerated due to velocity pull-up/pull-down effects; cf. Fig. 4a). The near-horizontal black lines in the velocity model (Fig. 4a) indicate inferred sources of wide-angle reflection phases recorded in the WARR dataset. The velocity model does not image any anomalous structure in the disrupted area nor does it resolve the Moho duplication imaged at km 100-110 (cf. Fig. 4a).

The crystalline crust (pink layer in Fig. 4b), between the Moho and the sedimentary layers, generally displays a reflective fabric. The least reflective segment is the uppermost crust in the northeast, above ~5 s, which can be considered as an almost transparent zone. Beneath the southern flank of the DF, separate zones characterised by distinct seismic fabrics are tentatively identified as suggested by the black dotted lines in Figure 4. In the southwesternmost part of the imaged crustal layer, reflectivity parallels the dipping basement surface in the uppermost crust and flattens towards the Moho. Across the inferred faults to the northeast of this zone, below the DF, reflectivity dips generally southwestward. Wide-angle reflected phases are observed in the WARR dataset coming from mid-crustal levels on both sides of the DF (near-horizontal black lines at a depth of 20-25 km in Figure 4a).

Beneath the axial part of the DF, the lower crust and the Moho are characterised by exceptionally strong reflectivity that corresponds to a lower crustal high-velocity layer identified by the refraction data (light green body; Fig. 4b). The high reflectivity in both normal incidence and wide-angle seismic datasets makes it likely that the body originates from magmatic processes, such as intrusion of mantle melts into the lower crust during Late Palaeozoic rifting (DOBREfraction'99 Working Group, 2003), such bodies being a common feature beneath rift basins elsewhere sometimes referred to as a "rift pillow" (e.g., Ervin and McGinnis, 1975; Mooney and Brocher, 1987).

Beneath the transparent upper crust of the northeastern flank of the DF, at TWT greater than about 5 s (Fig. 4b) in the reflection seismic image, equivalent to 15-20 km depth, the crystalline crust is strongly laminated and it is possible to distinguish zones having different seismic fabrics, here also separated by "fault zones" indicated by the dotted black lines in Figure 4b. These inferred structures are located in the area where the reflection Moho has been disrupted and can be extrapolated into the uppermost mantle; no formal interpretation of these inferred structures has ever been published.

4.2 Rocks and rock densities

The DOBRE seismic profiles provide the structural constraints for the upper mantle and crustal structural and compositional model across the DF segment of the DDB and the compositional constraints are provided by the DOBRE velocity model combined with densities derived from modelling gravity anomalies along the profile. Accordingly, appropriate relationships between seismic velocities and densities – for sedimentary rocks as well as crystalline rocks – were required for initial parameterisation of the upper mantle and crustal structural and compositional model.

A generalisation of published data on the distribution of values of P-wave velocity (V_p) and rock density (ρ) for crystalline (basement) rocks in the study area is listed in Table 1. In order to account for depth effects, a pressure of 0.1 GPa (roughly a depth ≤ 4 km) has been used for V_p≤6.4 km/s and a pressure of 0.5 GPa for higher velocities, representing the deeper levels of the crystalline crust. The observations summarised in Table 1 are plotted in Figure 5. One quantitative density-velocity relationship proposed for the VM and Ukrainian Shield (UkS) is that of Krasovsky (1981), shown as a solid line in Figure 5, and it is adopted in the present study except for rocks comprising the lower crust and uppermost mantle with velocities greater than 7.0 km/s. For these, an alternative relationship, proposed by Gordienko (1999), has been adopted (dashed line in Figure 5).

According to Golizdra and Popovich (1999), Palaeozoic sedimentary rocks of the DF typically have densities that are 0.05-0.1 Mg/m^3 higher than those given by standard conversion V_p-ρ functions for sediments such as Ludwig et al. (1971), and these are listed in Table 2. Observations are tabulated according to stratigraphic succession rather than rock type because depth of burial was observed to have greater influence than lithology. Rocks found in the DF were deeply buried prior to late Carboniferous-early Permian uplift along its southern margin and subsequent basin inversion events that culminated in the Late Cretaceous. Accordingly, they have densities that are as great as or even exceed the average density of the crystalline rocks of the Precambrian basement and, further, they display some lateral density variation with densities at a depth of 2 km on the southern margin, for example, being some 0.1-0.2 Mg/m^3 greater than those at the same depth on the northern margin. This is mainly the result of less compaction and consolidation to the north; corresponding density contrasts between equivalent strata on the north flank and the south flank decrease with depth (Golizdra and Popovich, 1999).

5. Upper mantle and crustal structural and compositional model

5.1 Modelling approach and added value

The definition of the final upper mantle and crustal structural and compositional model along the DOBRE profile, shown in Figure 6, was developed by first adopting an initial architecture constrained by the DOBRE seismic datasets (sub-section 4.1; Fig. 4) and a density distribution constrained by the empirical velocity-density relationships documented for the DF sedimentary fill and basement (sub-section 4.2; Fig. 5 and Tables 1 and 2). This process allowed some “smoothing” of the structural model but not exceeding velocity model

uncertainties (cf. DOBREfraction'99 Working Group, 2003), and this resulted in an initial model with a calculated gravity field that was broadly in good agreement with the observed gravity field. The final model seen in Figure 6a was achieved with additional minor perturbations to the initially adopted densities, all permissible within the uncertainties of the utilised density-velocity relationships. Figure 6b shows an integrated velocity-density model subdivided into main tectonic elements, including schematic crustal layering, with petrophysical attributes and, for schematic purposes only, "candidate" rock types linked to Figure 5 and Tables 1 and 2.

Since only a very few adjustments to the initial velocity/structural model were required to achieve a highly satisfactory gravity model, it follows that much of the crustal and upper mantle structure outlined in Figure 6 is basically consistent with the seismic interpretations described in section 4.1. This includes (1) the shape and thickness of the Palaeozoic and younger pre-, syn- and post-rift sedimentary succession; (2) the approximately flat Moho at 40 km and the high velocity/high density body ("rift pillow") asymmetrically underlying the rift basin and (3) the remainder of crystalline crust lying above the Moho and the "rift pillow" and below the sedimentary package. The first of these is exclusively the result of Palaeozoic rifting processes and the second is dominantly the result of Palaeozoic rifting processes so are not of primary interest in the present context of pre-existing features that localised Palaeozoic rifting.

However, as regards the third density-velocity model element, the crystalline crustal layer excluding the "rift pillow", the modelling has delivered added value to understanding the Precambrian, pre-rift crustal structure contiguous to the DDB. First, there is a low-density (in any case, less than ambient density) body in the upper crust beneath the northeastern flank of the DF and, second, there are clearly contrasting velocity-depth (and density-depth) relationships on either side of the DF. Both of these are of potential relevance to the question of rift localisation in this part of Sarmatia and are further described in the following sections.

5.2 Low velocity upper crust beneath the northeastern flank of the DF

The gravity low over the northeastern flank of the DF, centred approximately on the surface trace of the crustal thrust zone (~km 230-235) and approximately coinciding with the thin layer of low velocity sediments, can only be explained by reducing densities in the upper crystalline crust (below the sedimentary succession). In the final model, this is implemented with a body of a uniform density of 2.67 Mg/m^3 descending from the base of the DF to a depth of about 18 km (Fig. 6). No permissible adjustments to the model involving density or

structural “tweaks” to the supracrustal sedimentary successions can aid in explaining the negative gravity anomaly, a conclusion that was also reached by Yegorova and Kozlenko (2003) and Lyngsie et al. (2007).

The DOBRE WARR velocity forward modelling did not explicitly reveal anomalously lower velocities in the upper crust in this region although a preliminary tomographic inversion of first seismic arrivals in the DOBRE WARR dataset did suggest a subtle low velocity zone in this area (DOBREfraction’99 Working Group, 2003). The inferred extent of the low-density body in the gravity model is also roughly coincident with the most transparent upper crust of the deep seismic reflection image (Fig. 4b). Accordingly, the presence of a (relatively) low-velocity body filling most of the upper crust beneath the northern flank of the DF is a robust element of the model. Examination of both velocities and densities (Fig. 6b) suggests that this body comprises strongly granitised upper crust or possibly a rather homogeneous granitic intrusion (Fig. 5). This is also in keeping with what is known of the basement geology of this area (Fig. 3), where Paleoproterozoic granites and migmatites are widely reported.

5.3 Contrasting density/velocity depth character across the DF

The crystalline crust layer displays higher velocities and densities beneath the AM to the southwest of the DF than beneath the VM to its northeast (Fig. 6) and this is demonstrated in Figure 7 at the locations indicated by arrows in Figure 6a. This occurs throughout the crust as a whole although, as seen in the final density model (Fig. 6a), it is enhanced by a thin (~5 km) high density layer in the lowermost crust, immediately above the Moho, which has been assigned the same densities as the contiguous high velocity lower crustal “rift pillow”. The disposition of this layer correlates with the thin high reflectivity zone lying above the AM Moho in the DOBREflection image (Fig. 4b), which has similar properties as the “rift pillow” segment, but is absent northeast of it beneath the VM. The difference in the crustal density structure on either side of the rift zone is responsible for the regional gravity background trend of the study area, which along the DOBRE profile is expressed as a northeastward decrease from 40 mGal to 20 mGal (Fig. 6a). The thin high-density layer at the base of the AM crust partly balances a countervailing trend in the upper mantle, where velocities, well-constrained by the WARR data (Fig. 4a), increase from southwest to northeast (8.0 to 8.3 km/s) with similarly trending densities inferred accordingly (3.39 to 3.43 Mg/m^3; Fig. 6).

The compositional layering in the integrated-petrological version of the density model in Figure 6b should be taken as schematic only and certainly not definitive in any way, but it illustrates one way of viewing the crustal differences between the AM crust contiguous to the

DF, to the southwest, and the VM contiguous to the DF, to the northeast. In this representation, the VM crust consists of two layers. The upper crustal layer has bulk velocities and densities that are typical of granitic or migmatitic rocks, as mapped at basement level (Fig. 2), including the large proportion of it occupied by the low-density granitic body mentioned above. The wide-angle reflecting horizon at about 25 km depth in the WARR seismic image (Fig. 4a) is adopted as the "boundary" of the seismically transparent upper crustal layer with the underlying lower crustal layer. The lower crustal layer displays more reflectivity (Fig. 4b) and, in terms of its geophysical attributes, is not dissimilar to the average middle continental crustal layer as compiled by Christensen and Mooney (1995), being a bit more mafic than the layer above. The AM crust also consists of two layers (excluding the thin high-velocity layer at the base of the crust) but the upper crustal layer is much thinner (<10 km versus >20 km) and the middle-lower crustal layer is much thicker (>25 km versus <20 km) than observed in the VM crust.

6. Discussion: Precambrian structural control on Late Palaeozoic rifting

6.1 Contrasting crustal affinity across the DDB rift

The main element of the pre-DF structural-compositional model (Fig. 6) that may be relevant to the localisation of DDB rifting in the Late Palaeozoic is the marked contrast in velocity/density structure of AM crust to the southwest and VM crust to the northwest, as this is a pre-rift, Precambrian-aged feature. It is graphically expressed very clearly in Figures 5 and 7. Bulk V_p/V_s ratios are also slightly higher in AM crust than VM (though the difference, 1.75 versus 1.73, may not be significant; DOBREfraction'99 Working Group, 2003). It is further noted that the upper mantle below the AM crust is also different from the upper mantle below the VM crust, the former having lower velocity and density (8.0-8.1 km/s and 3.39 Mg/m^3) than the latter (8.3 km/s and 3.43 Mg/m^3).

Gravity modelling by Starostenko et al (2008) along the DOBRE profile also found a lower crustal mean density on the VM side of the DF compared to the AM side although these authors' final model did not honour several robust constraints common to both the DOBRE WARR and reflection results, including the location of the sedimentary basement surface. In contrast, closely following the DOBRE constraints, Lyngsie et al. (2007) considered that the crust on either side of the DF was essentially the same, the only difference being limited to the presence of a high-density layer in the lowermost AM crust, which they attributed to intrusion of ultramafic material associated with Late Palaeozoic rifting. Lyngsie et al. (2007),

however, adopted the widely used velocity-density relation of Barton (1986), which is not optimal for the observed attributes of the rocks occurring in the study area, as compiled in Figure 5.

In the present study the extra mass on the southwestern flank of the rift is distributed throughout the crust and is responsible for higher background Bouguer anomalies to the southwest of the rift axis compared to those than to the northeast. The regional gravity field shows that this is not a phenomenon limited to the vicinity of the DOBRE cross-section and, therefore, not a consequence of post-rift Permian tectonism (e.g., DOBREfraction'99, 2003), the geological effects of which are seen only on the southern margin of the DF. It can be seen in Figure 3a that regional gravity anomalies over the Ukrainian Shield and Azov Massif are typically in the range ~+20 – +30 mGal compared to ~-20 – -40 mGal over the Voronezh Massif. There is indeed a dramatic difference in the general level of the gravity field on either side of the DDB along much of its length from the DF to its Dniepr segment to the northwest. This effect is also clearly seen in the residual gravity anomaly field across this region calculated by Yegorova et al. (1999) by removing the gravity effects of sedimentary strata and a crust of uniform density from the observed field, which is some 50 mGal higher to the southwest of the rift than to the northeast.

Shchipansky and Bogdanova (1999) considered that the Sarmatian basement trends and tectonic domains southwest and northeast of the DDB could be correlated such that they cut across the trend of the younger rift. With respect to the DF specifically they correlated the Oskol block to the northeast with the Azov block to the southwest, referring to it as one composite Oskol-Azov block, as seen in Figure 1 and with its western boundary indicated on Figure 3. Both the Oskol and Azov blocks are mapped as "Archaean-Palaeoproterozoic undivided" and Shchipansky and Bogdanova (1999) are clear that a "persisting absence of detailed field and geochronological data" (p. 114) makes it difficult to distinguish retrograde high-grade Archaean rocks from Palaeoproterozoic supracrustals. They caution that the Oskol-Azov block may not be a single, coherent tectonic unit but could be an assemblage of terranes with different tectonic histories and ages. Later, Bogdanova et al. (2001) showed a schematic model that included Palaeoproterozoic "accretionary growth rims" (p. viii) between Sarmatia and Volgo-Uralia, equivalent to the unit lying between the Oskol-Azov block and the Volgo-Donets orogen in Figure 1. Given the proximity of the northern part of the DOBRE profile to this unit, it cannot be ruled out that the Oskol-Azov block in this area was overprinted by processes linked to the suturing of Sarmatia with Volgo-Uralia at 2.1-2.0 Ga but not further south.

While the DOBRE data demonstrate that Moho depth is roughly constant at about 40 km on either side of the DF, they also show that seismic fabric and velocity structure of the crystalline basement at either end of the DOBRE profile are somewhat dissimilar. The gravity field modelled in the light of the DOBRE seismic constraints provides a compelling argument that the crustal structure on either side of the DDB may well an expression of contrasting tectonic affinities (and, hence, differing tectonic histories) and that the rift zone may coincide with the locus of a suture between distinct tectonic blocks as highlighted by Shchipansky and Bogdanova (1999). Regarding the observed shift in background gravity level across the DDB, regional sutures within the North American craton in Canada were recognised long ago as being marked by similar gravity signatures (Thomas and Tanner, 1975; Gibb and Thomas, 1976). In Canada, however, these are not in part obliterated or strongly overprinted by Phanerozoic rifting, magmatism, basin formation and inversion as for the DDB.

That a suture (of sorts) or some kind of zone of crustal weakness underlies and influences the siting of the DDB (though not confined to Sarmatia or even a part of it) is not a new idea. Pre-plate tectonics models had the DDB as part of a continent-scale linear zone of weakness, developed at the surface by various structures including sedimentary basins, running from Poland to the Turanian Plate, east of the Caspian Sea (e.g., Aizberg et al., 1971; Chekunov, 1994). Related to this was a long-held idea that the DDB developed atop a Proterozoic aulacogen or paleorift (e.g., Chekunov et al., 1992), though Stovba et al. (1996) demonstrated convincingly that no such Proterozoic basin underlies the DDB (and, similarly, this is also seen on DOBRE in the DF segment; cf. Fig. 4).

6.2 The dynamics of DDB rifting

The considerations discussed above lean towards a model where Precambrian crustal/lithospheric structure has influenced Late Palaeozoic rifting across Sarmatia. Such thinking is usually in terms of a pre-existing “zone of weakness” but what actually constitutes a “zone of weakness” for reactivation hundreds of millions of years after its initial formation? The very existence of an inherited “suture” or crustal scale structure within the lithosphere is typically regarded as sufficient to imply a “zone of weakness”. Rifting models (whether analogue, numerical or qualitative) necessarily possess heterogeneities with properties weaker than ambient materials in order to seed the initiation of rifting (e.g., Huismans and Beaumont, 2007). The long-lived persistence of such heterogeneities in the real Earth is generally accepted (e.g., Heron et al., 2016a).

Regarding long-lived "frozen-in" structural heterogeneity, the DOBRE crust and upper mantle model presented in the present study does not reveal any explicit evidence. Nor is there is any evidence, certainly no diagnostic evidence, for the presence of a pre-Palaeozoic aulacogen, which could be considered a proxy for inherited structural heterogeneity. The DOBRE profile, however, images only the crust and the uppermost mantle (including several wide-angle reflecting horizons within the latter) whereas Heron et al. (2016b) have recently argued that deeper structures within the continental mantle lithosphere could be more important than crust-only heterogeneities for localising and controlling later tectonic reactivations. Mantle-embedded heterogeneities would include fossil suture zones and similar but the DOBRE data do not have the capability of confidently imaging them. Various kinds of focused, purpose-built surveys using passive seismological methodologies could help with this, providing information to test the hypothesis of there being a Precambrian lithospheric structural heterogeneity guiding the eventual location of the DDB rift.

Having an inherited structural heterogeneity or "zone of weakness" is not in itself sufficient to later produce an intracratonic rift zone; it will also be necessary to have the right kind of intraplate tectonic stress field – orientated favourably as well as large enough – to result in its reactivation. The "right kind" of intraplate tectonic stress field consists in part by stresses generated by "tectonic" forces, caused by whatever geodynamic process is driving rifting, and in part by those derived from variations in geopotential energy (GPE) of the lithosphere (e.g., Coblentz et al., 1994; Nielsen et al., 2014; Stephenson et al., 2020). GPE is defined as the integrated lithostatic pressure in a given rock column and varies from place to place depending on density variations within the lithosphere, including variations in topography, laterally varying crustal structure, including sediment thickness and Moho depth, and lithosphere thickness (e.g., Schiffer and Nielsen, 2016). For example, the "pressure (40 km depth)" curve plotted on Figure 6a is representative of the component of GPE caused by lateral density variations within the crust along the DOBRE profile. This excludes contributions from topography along the profile, which are, in any case, minimal and do not display any striking correlation with the pressure anomaly (Fig. 6a).

The GPE-derived intraplate stress field can be considered the stable, background stress field to which stresses caused by transient tectonic forces are added if and when nearby plate boundaries are subject to geodynamic processes such as subduction or plate boundary reconfigurations or if dynamic forces from the underlying asthenosphere are imposed. If the superposition of these two stress field components results in favourable interference producing extensional stresses in the right orientation and of sufficient magnitude to exceed

the strength of the lithosphere then intraplate deformation – such as in the Late Devonian, when rifting occurred in the DDB – occurs (whether in the presence of inherited structure or not, though it may play a role).

In this context, there are two Precambrian basement features defined in the present work that may be relevant to a localised stress field aligned with the eventual axis of Late Devonian rifting within Sarmatia. The first is the northeast-decreasing gravity gradient across the DDB, perpendicular to its axis. It is not possible to say with certainty from the DOBRE profile results that the density distribution within the crystalline crust causing this gravity gradient is inherited from pre-rift times although it seems more likely to be the case than not. The gravity gradient means that there is also a gradient in GPE perpendicular to the rift axis (e.g., proxied as "pressure" in Fig. 6a) and, in turn, a perturbation in the GPE-derived stress field associated with the rift axis. The second feature is the upper crustal low-density granite body, and its negative gravity signature, below the northeastern flank of the DF. The mass deficiency related to this body compared to contiguous crust contributes to the pressure anomaly seen in Figure 6. It is also possible that another gravity low seen on Figure 3a further along the DDB rift margin to the northwest (around 35° longitude, 50° latitude), of similar appearance and amplitude, could indicate a second such granitic body, together suggesting an alignment with the DDB rift orientation.

The horizontal deviatoric stress along the profile is directly related to the horizontal gradient of the pressure curve in Figure 6a caused by the lateral density variations in the underlying crust (e.g., Coblentz et al, 1994; Turcotte and Schubert, 2002; Schiffer and Nielsen, 2016; cf. Artyushkov, 1973). The actual magnitude and sign of this depends on adopting a reference lithosphere model but, in general, the horizontal deviatoric stress will become more extensional in the direction of lower pressure (~GPE) values and, accordingly, will be relatively extensional where there exists a low-pressure anomaly. Order of magnitude calculations suggest that these GPE-generated extensional horizontal deviatoric stresses are in the range 10-20 MPa in the crust of the DOBRE profile in the area of the gravity low. This is a similar magnitude to those computed regionally, but more rigorously, in plate-scale structural models (e.g., Nielsen et al., 2014; Schiffer and Nielsen, 2016; Stephenson et al., 2020). Such a magnitude is less than the strength of the crust computed for cold, cratonic lithosphere on the basis of maximum shear stress in rheological strength diagrams (e.g., Ranalli and Murphy, 1987; cf. Beekman et al., 1997), which are typically greater than 100 MPa for crustal depths. Nevertheless, in the presence of a favourably-orientated, extensional

(tectonic) stress field, such a 10-20 MPa perturbation may provide a sufficient contribution to the total intraplate stress field to drive deformation.

Zonenshain et al. (1990) considered the DDB rift to be a failed arm of a rift system that led to the Late Palaeozoic development of a system of small ocean basins, subsequently closed, along the southern margin of the EEC. In this scenario the DDB had a common geographic termination with the contemporaneous Peri-Caspian Basin (Brunet et al., 1999) that was an ("oceanic") arm of the same rift-rift-rift system but Zonenshain et al. (1990) did not speculate what constituted the third arm. Because of severe Mesozoic-Cenozoic tectonic overprinting it remains highly uncertain whether such a third arm existed and how it might be recorded in the present-day geology of the Alpine-Tethys orogenic belt in this area. According to the middle-late Devonian tectonic reconstructions of Stampfli and Kozur (2006) and Stampfli et al. (2013), the third arm of a "Zonenshain" triple-rift system could be what these authors called the Paphlagonian Ocean, the geological record of which may be in northern Turkey and the Transcaucasus area (between the Black and Caspian seas). It may have formed an eastern prolongation of the Rheno-Hercynian Ocean that is recorded in the geology of the Variscan orogen in central Europe (e.g., Franke, 2006). The "Zonenshain" triple-rift is shown schematically on the inset map of Figure 1.

The tenets of plate tectonics hold that stresses caused by a domal uplift are most efficiently relaxed along three fractures at roughly 120°, hence forming a rift-rift-rift triple junction. A number of different kinds of geological studies, mentioned in section 2 above, document that the intensity of rifting during formation of the DDB increased to the southeast through the DF segment and that mantle thermal processes and concomitant uplift probably played an increasingly important role in this direction (cf. Stephenson et al., 2006). In this regard, Puchkov et al. (2016) suggested the DDB could be linked to a mantle plume centred further to the southeast of its termination than envisaged by Zonenshain et al (1990) and manifest as part of an EEC-wide "Kola-Dnieper" Large Igneous Province (Ernst, 2014).

7. Summary and conclusions

An investigation of factors that might guide rifting within cold, intracratonic lithosphere has been carried out as a case study of the geophysically well-constrained crustal structure of the Donbas Foldbelt (DF) and surrounding basement geology in southeastern Ukraine. The DF is the southeastern and thickest segment of the Dniepr-Donets Basin (DDB) rift, which formed in the Late Devonian in an intracratonic setting but near and at a highly oblique angle to the

tectonically-active southern margin of the Laurasian proto-continent (Baltica component) at that time. The main conclusions and considerations resulting from the investigation follow.

(1) A robust compositional-structural model of the crust and upper mantle has been made on the basis of excellent gravity data, extensive petrological observations constraining rock velocities and densities, and controlled by the coincident DOBRE wide-angle reflection and refraction and deep near-vertical seismic reflection surveying. It was possible to distinguish those elements in the crustal model that existing prior to rifting in the Late Palaeozoic from modifications caused by rifting and later tectonic events and, therefore, to consider these in terms of how DDB rifting was "seeded".

(2) There appear to be significant differences in the structure of the pre-rift cratonic crust on either side of the DF – the Azov Massif, to the south, and the Voronezh Massif to the north. This is expressed by higher velocities and densities in the crust in the former than in the latter. Regional gravity trends suggest that these differences can be extrapolated from the DF to the northwest along the entire extent of the DDB. These differences may be inherent to the accretionary processes that formed Sarmatia in the Archaean and Paleoproterozoic and speak against a model of Sarmatian structural continuity across the superimposed DDB-DF rift zone. However, there is no revealed evidence in the present study for a crustal-scale suture or other kind of structural heterogeneity within the crust and/or upper mantle. Further, it cannot be categorically ruled out that the inferred contrast in crustal architecture was not caused by subsequent tectonic overprinting events: first, the Late Devonian rifting event itself and, second, Permian tectonics expressed by significant uplift of the southern margin of the DF.

(3) A large, homogeneous, upper crustal low-density granitic body of Archaean-Palaeoroterozoic age lies beneath the northeastern flank of the DF and the regional gravity field suggests that there may be a similar such body adjacent to the Dniepr segment of the DDB along strike to the northwest of the DF. These inferred granitic bodies are characterised by significant negative gravity anomalies superimposed on the gravity gradient produced by the crustal structure contrast across the DDB-DF. The gravity gradient together with the superimposed gravity lows imply the presence of a gravitational potential energy deficiency that produces extensional (relative to some reference stress field) horizontal deviatoric stresses perpendicular to the trace of the DDB. The magnitude of these stresses is of the order of those produced by gravitational potential energy variations in intraplate lithosphere generally. Accordingly, they could represent a meaningful, extensionally favourable,

perturbation to the ambient stress field in the presence of stresses generated by other active, transient, tectonic processes affecting the EEC lithosphere in this area in the Late Devonian.

(4) It is hypothesised that the DDB rift formed as part of a complex rift system on the southern margin of Laurasia in the Late Devonian that included the Peri-Caspian Basin to the northeast and possibly the Rheno-Hercynian Ocean to the south-southwest (present-day geographic reference), the latter being closed during the subsequent Variscan Orogeny. This does not necessarily imply that there is a crustal scale boundary or structural heterogeneity that guided DDB rifting. However, if the DDB rift is indeed a failed arm of a Late Devonian rift-rift-rift system then it seems likely its location within the East European Craton may have been influenced by the stress-perturbing factors identified in this study.

(5) It cannot be concluded with certainty that either inherited structural weakness or a superimposed favourable geopotential stress field was necessary or sufficient for "seeding" Late Palaeozoic rifting in Sarmatia but modern passive seismology surveys across the DDB as well as new bedrock geological studies including geochronology would help test such a hypothesis.

Acknowledgements

Svetlana Bogdanova was a very active participant of EUROPROBE, a programme of the European Science Foundation aimed at pooling expertise and enhancing communication, scientific and within friendships, between western European solid Earth scientists and those in countries opening up in eastern Europe and the former Soviet Union. Svetlana was at the founding meeting of EUROPROBE in Jabłonna near Warszawa in Poland in 1991 and is fondly remembered by RS as a storming presence, a force of nature, at that meeting. RS also had the great privilege of co-editing with Svetlana and her husband Roland Grobatschev a special issue of *Tectonophysics* (volume 339, 2001) based on the Eurobridge project within EUROPROBE. The DOBRE project discussed at length in this paper and its multitude of ancillary geological, geophysical and geochemical studies that have also been mentioned, and many others as well, took place under the EUROPROBE umbrella. Finally, the generous efforts of two anonymous reviewers of an earlier version of this manuscript are much appreciated by the authors and have resulted in significant improvements.

References

Aizberg, R.E., Garetskij, R.G. and A.M. Sinichka (1971), Sarmatsko-Turanian lineament of the Earth's crust, in: *Problems of Theoretical and Regional Tectonics*, edited by A.V. Peive, pp.41-51, Nauka, Moscow (in Russian).

Alexandre, P., Chalot-Prat, F., Saintot, A., Wijbrans, J., Stephenson, R., Wilson, M., Kitchka, A. and Stovba, S. (2004), The $^{40}Ar/^{39}Ar$ dating of magmatic activity in the Donbas Fold Belt and the Scythian Platform (Eastern European Craton), *Tectonics, 23*, TC5002, doi:10.1029/2003TC001582.

Artyushkov, E.V. (1973), Stresses in the lithosphere caused by crustal thickness inhomogeneities, *J. Geophys. Res., 78*, 7675-7708.

Barton, P.J. (1986), The relationship between seismic velocity and density in the continental crust – a useful constraint? *Geophys. J. R. astr. Soc., 87*, 195-208.

Barrier, E., Vrielynck, B., Brouillet, J.F. and Brunet, M.F. (2018), Paleotectonic Reconstruction of the Central Tethyan Realm. In: Tectono-Sedimentary-Palinspastic maps from Late Permian to Pliocene. CCGM/CGMW, Paris. http://www.ccgm.org (Contributors: Angiolini, L., Kaveh, F., Plunder, A., Poisson, A., Pourteau, A., Robertson, A., Shekawat, R., Sosson, M. and Zanchi, A.) (Atlas of 20 maps (scale: 1/15 000 000)).

Beekman, F., Stephenson, R.A. and Korsch, R.J. (1997), Mechanical stability of the Redbank Thrust Zone, Central Australia: Dynamic and rheological implications, *Australian Journal of Earth Sciences, 44*, 215-226. doi:10.1080/08120099708728305

Bogdanova, S. (1993), The three-segment hypothesis for the East European Craton (Abstract), *Terra Nova, 5*, 313.

Bogdanova, S.V., Bingen, B., Gorbatschev, R., Kheraskova, T.N., Kozlov, V.I., Puchkov, V.N. and Volozh, Yu.A. (2008), The East European Craton (Baltica) before and during the assembly of Rodinia, *Precambrian Research, 160*, 23-45. doi:10.1016/j.precamres.2007.04.024

Bogdanova, S.V., Gorbatschev, R. and Garetsky, R.G. (2016), EUROPE | East European Craton, Reference Module in Earth Systems and Environmental Sciences, Elsevier. doi: 10.1016/B978-0-12-409548-9.10020-X.

Bogdanova, S.V., Gorbatschev, R. and Stephenson R.A. (2001), EUROBRIDGE: Palaeoproterozoic accretion of Fennoscandia and Sarmatia – preface, *Tectonophysics, 339*, vii-x.

Brunet, M.F., Volozh, Yu.A., Antipov, M.P. and Lobkovsky, L.I. (1999), The geodynamic evolution of the Precaspian Basin (Kazakhstan) along a north-south section, *Tectonophysics, 313*, 85-106.

Buck, W.R. (1991), Modes of continental lithospheric extension, *Journal of Geophysical Research, 96*, 20161-20178.

760 Chekunov, A.V. (1994), The geodynamics of the Dnieper-Donets syneclise, *Geophysical*
761 *Journal, 16*(3), 3-13 (in Russian).
762
763 Chekunov, A.V., Gavrish, V.K., Kutas, R.I. and Ryabchun, L.I. (1992), Dnieper-Donets
764 palaeorift, *Tectonophysics, 208,* 257-272.
765
766 Chirvinskaya, M.V. and Sollogub, V.B. (1980), Deep structure of the Dniepr-Donets
767 aulacogen from geophysical data. Kiev: Naukova Dumka, 178 pp. (in Russian).
768
769 Christensen, M.I. and Mooney, W.D. (1995), Seismic velocity structure and composition of
770 the continental crust: A global view, *J. Geophys. Res., 100,* 9761-9788.
771
772 Coblentz, D.D., Richardson, R.M., Sandiford, M. (1994), On the gravitational potential of the
773 Earth's lithosphere, *Tectonics, 13*, 929-945.
774
775 Currie, C.A., Huismans, R.C. and Beaumont, C. (2008), Thinning of continental backarc
776 lithosphere by flow-induced gravitational instability, *Earth Planet. Sci. Lett., 269*, 436-447.
777
778 Currie, C.A. and Hyndman, R.D. (2006), The thermal structure of subduction zone back arcs,
779 *J. Geophys. Res. 111,* B08404. doi:10.1029/2005JB004024
780
781 Danišík, M., Sachsenhofer, R.F., Privalov, V.A., Panova, E.A., Frisch, W., Spiegel, C. (2008),
782 Low-temperature thermal evolution of the Azov Massif (Ukrainian Shield-Ukraine) –
783 Implications for interpreting (U-Th)/He and fission track ages from cratons, *Tectonophysics,*
784 *456*, 171-179.
785
786 DOBREfraction'99 Working Group (2003), "DOBREfraction'99", velocity model of the
787 crust and upper mantle beneath the Donbas Foldbelt (east Ukraine), *Tectonophysics, 371,* 81-
788 110.
789
790 Ernst, R.E. (2014), *Large igneous Provinces*. Cambridge University Press, Cambridge, 653 p.
791
792 Ervin, C.P. and McGinnis, L.D. (1975), Reelfoot rift: reactivated precursor to the Mississippi
793 Embayment, *Geol. Soc. Amer. Bull., 86*, 1287-1295.
794
795 Franke, W. (2006), The Variscan orogen in Central Europe: construction and collapse, in
796 European Lithosphere Dynamics, edited by D.G. Gee and R.A. Stephenson, pp. 333-343,
797 Geological Society of London, Memoir 32.
798
799 Garkalenko, I.A., Borodulin, M.I. and A.K. Michalev (1971), About the transition zone
800 between the Dnieper-Donets Basin and Donets folded structure, *Geological Journal, 31*, 92-
801 98 (in Russian).
802
803 Gavrish, V.K. (1989), *Geology and Oil and Gas Potential of the Dniepr-Donets Depression:*
804 *Depth Structure and Geotectonic Evolution*, 208 pp., Naukova Dumka, Kiev (in Russian).
805
806 Gee, D.G. and Stephenson, R.A. (2006), The European lithosphere: an introduction, in
807 European Lithosphere Dynamics, edited by D.G. Gee and R.A. Stephenson, pp. 1-9,
808 Geological Society of London, Memoir 32.
809

Gibb, R.A. and Thomas, M.D. (1976), Gravity signature of fossil plate boundaries in the Canadian Shield, *Nature, 262,* 199-200.

Golizdra, G.Ya. and Akhmetshina, A.K. (1973), About the sources of regional gravity highs of Azov region, *Geophysical sbornik, 51,* 69-77.

Golizdra, G.Ya, and Popovich, V.S. (1999), Density models of sedimentary strata of the SE DDD, western and northern margins of Donbas, *Geophysical Journal, 18,* 1263-1274.

Gorbatschev, R. and Bogdanova, S. (1993), Frontiers in the Baltic Shield, *Precambrian Res., 64,* 3-22.

Gordienko, V.V. (1999), *Density Models of the Tectonosphere of the Territory of the Ukraine,* 100 pp., Intellect, Kiev (in Russian).

Gordienko, V.V and Usenko, O.V. (2003), *Deep Processes in the Tectosphere of Ukraine,* 147 pp., Kiev (in Russian).

Heron, P.J., Pysklywec, R.N. and Stephenson, R. (2016a), Lasting mantle scars lead to perennial plate tectonics, *Nature Communications, 7,* 11834. doi:10.1038/ncomms11834

Heron, P.J., Pysklywec, R.N. and Stephenson, R. (2016b), Identifying mantle lithosphere inheritance in controlling intraplate orogenesis, *Journal of Geophysical Research, Solid Earth, 121,* 6966-6987. doi:10.1002/2016JB013460

Huismans, R.S. and Beaumont, C. (2007), Roles of lithospheric strain softening and heterogeneity in determining the geometry of rifts and continental margins. Geological Society, London, Special Publications, 282, 111-138. doi:10.1144/SP282.6

Kabyshev, B., Krivchenkov, B., Stovba, S. and Ziegler, P.A. (1998), Hydrocarbon habitat in the Dniepr-Donets Depression, *Marine and Petroleum Geology, 15,* 177-190.

Khain, V.E. and Leonov, Yu.G., eds. (1996), International Tectonic Map of Europe, 3rd edition (1:5,000,000). Commission for the Geological Map of the World.

Krasovsky, S.S. (1981), *Reflection of Continental-type Crustal Dynamics in the Gravity Field,* 264 pp., Naukova dumka, Kiev (in Russian).

Kusznir, N.J., Stovba, S.M, Stephenson, R.A. and Poplavskii, K.N. (1996), The formation of the northwestern Dnieper-Donets Basin: 2-D forward and reverse syn-rift and post-rift modelling, *Tectonophysics, 268,* 237-256.

Lebedev, T.S., Korchin, V.A., Savenko, B.Ya., Shapoval, V.I. and Shepel', S.I. (1986), Physical Properties of Mineral Matter in Temperature-Pressure Conditions, 193 pp., Naukova Dumka, Kiev (in Russian).

Ludwig, W.I., Nafe, J.E. and Drake, C.L. (1971), Seismic refraction, in *The Sea vol.4,* edited by A.E. Maxwell, pp. 53-84, John Wiley & Sons, New York.

Lyngsie, S.B., Thybo, H. and Lang, R. (2007), Rifting and lower crustal reflectivity: A case study of the intracratonic Dniepr-Donets rift zone, Ukraine, *J. Geophys. Res.*, *112*, B12402, doi:10.1029/2006JB004795.

Maystrenko, Yu., Stovba, S., Stephenson, R., Bayer, U., Menyoli, E., Gajewski, D., Huebscher, C., Rabbel, W., Saintot, A., Starostenko, V., Thybo, H. and Tolkunov, A. (2003), Crustal-scale pop-up structure in cratonic lithosphere: DOBRE deep seismic reflection study of the Donbas Foldbelt, Ukraine, *Geology, 31,* 733-736.

Meijers, M.J.M., Hamers, M.F., van Hinsbergen, D.J.J., van der Meer, D.G., Kitchka A.A., Stephenson, R.A. and Langereis, C.G. (2010), New late Paleozoic paleopoles from the Donbas Foldbelt (Ukraine): implications for the Pangea A vs. B controversy, *Earth and Planetary Science Letters, 297*, 18-33. doi:10.1016/j.epsl.2010.05.028

Mitrovica, J.X., Pysklywec, R.N., Beaumont, C. and Rutty, A. (1996), The Devonian to Permian sedimentation of the Russian Platform: an example of subduction controlled long-wavelength tilting of continents, *J. Geodynamics*, *22*, 79-96.

Mooney, W.D. and Brocher, T. (1987), Coincident seismic reflection/refraction studies of the continental lithosphere, *Rev. Geophys., 25*, 723-742.

Muttoni, G., Kent, D.V., Garzanti, E., Brack, P., Abrahamsen, N. and Gaetani, M. (2003), Early Permian Pangea 'B' to Late Permian Pangea 'A', *Earth Planet. Sci. Lett., 215*, 379-394.

Nechayeva, T.S., Shymkiv, L.M. and Yentin, V.A. (2002). Scheme of the gravity field of Ukraine. PDRGP "Pivnichukrheolohiya" Publ., Kyiv (in Ukrainian).

Nielsen, S.B., Stephenson, R. and Schiffer, C. (2014), Deep controls on intraplate basin inversion (Chapter 10), in: Talwani, P. (Ed.), Intraplate Earthquakes. Cambridge University Press, pp. 257-274.

Pogrebnov, N.I., Ocheretenko, I.A., and Trostchenko, V.V. (1985), Subsurface-contour map of pre-Mesozoic deposits of Donets coal basin: Ministry of Geology of USSR, 3 sheets, scale 1: 500,000, 149 pp. (in Russian).

Poplavskii, K.N., Podladchikov, Yu.Yu. and Stephenson, R.A. (2001), Two-dimensional inverse modeling of sedimentary basin subsidence, *J. Geophys. Res., 106(B4)*, 6657-6672.

Popov, V.S. (1963), Tectonics of the Donets Basin, in Kuznetsov, I.A., ed., Geology of coal and oil shale deposits of the USSR, Volume 1: Moscow, Nedra, 103-151 (in Russian).

Popov, V.S. (1965a), The geological map of pre-Mesozoic sediments of the Ukrainian part of the Great Donbas: Ministry of Geology of USSR, 1 sheet, scale 1:500,000 (in Russian).

Popov, V.S. (1965b), The geological map of the pre-Cainozoic sediments of the Ukrainian part of the Great Donbas: Ministry of Geology of USSR, 1 sheet, scale 1:500,000 (in Russian).

Puchkov, V., Ernst, R.E., Hamilton, M.A., Söderlund, U. and Sergeeva, N. (2016), A Devonian >2000-km long dolerite swarm-belt and associated basalts along the Urals-

Novozemelian fold-belt: part of an East-European (Baltica) LIP tracing the Tuzo Superswell. *GFF, 138,* 6-16, doi:10.1080/11035897.2015.1118406

Ranalli, G. and Murphy, D.C. (1987), Rheological stratification of the lithosphere, *Tectonophysics, 132,* 281-295.

Saintot, A., Stephenson, R., Brem, A., Stovba, S. and Privalov, V. (2003a), Palaeostress field reconstruction and revised tectonic history of the Donbas fold-and-thrust belt (Ukraine and Russia), *Tectonics, 22,* 1059, doi:10.1029/2002TC001366.

Saintot, A., Stephenson, R.A., Stovba, S.M. and Maystrenko, Yu. (2003b), Structures associated with inversion of the Donbas Foldbelt, *Tectonophysics, 373,* 181-207.

Saintot, A., Stephenson, R.A., Stovba, S., Brunet, M-F., Yegorova, T. and Starostenko, V. (2006), The south margin of the East European continent: its evolution during the Palaeozoic and Early Mesozoic, in *European Lithosphere Dynamics,* edited by D.G. Gee and R.A. Stephenson, pp. 481-505, Geological Society of London, Memoir 32.

Schellart, W.P. (2009), Evolution of the slab bending radius and the bending dissipation in three-dimensional subduction models with a variable slab to upper mantle viscosity ratio. *Earth Planet. Sci. Lett., 288,* 309-319.

Schiffer, C. and Nielsen, S.B. (2016), Implications for anomalous mantle pressure and dynamic topography from lithospheric stress patterns in the North Atlantic Realm, *J. Geodyn., 98,* 53-69. doi:10.1016/j.jog.2016.03.014.

Shchipansky, A. and Bogdanova, S. (1996), The Sarmatian crustal segment: Precambrian correlation between the Voronezh Massif and the Ukrainian Shield across the Dniepr-Donets Aulacogen, *Tectonophysics, 268,* 109-126.

Sobornov, K. (1995), Structural evolution of the Karpinsky Swell, Russia, *Comptes Rendus de l'Acadimic des Sciences, Série IIa, 321,* 161-169.

Stampfli, G.M., Hochard, C., Vérard, C., Wilhem, C. and von Raumer, J. (2013), The formation of Pangea, *Tectonophysics, 593,* 1-19. doi:10.1016/j.tecto.2013.02.037

Stampfli, G.M. and Kozur, H.W. (2006), Europe from the Variscan to the Alpine cycles, in European Lithosphere Dynamics, edited by D.G. Gee and R.A. Stephenson, pp. 57-82, Geological Society of London, Memoir 32.

Starostenko, V.I, Danilenko, V.A., Vengrovitch, D.B., Kutas, R.I, Stovba, S.M, Stephenson, R.A. and Kharitonov, O.M. (1999), A new geodynamical-thermal model of rift evolution, with application to the Dnieper-Donets Basin, Ukraine, *Tectonophysics, 313,* 29-40.

Starostenko, V.I., Kozlenko, V.G., Oganesyan, S.M., Shen, E.L., Oganesyan, M.G., Yegorova, T.P. and Dyadura, G.V. (1990), Three-dimensional density distribution in the Dniepr Graben crust, *Geophysical Journal, 8*(6), 719-739.

Starostenko, V.I., Kuprienko, P.Yu., Makarenko, I.B. and Legostaeva, O.V. (2008), Density model of the Earth's crust along the profile DOBRE, *Geophysical Journal, 30(1),* 28-41.

960 Stephenson, R. (1996), Assumptions and observations in tectonic modelling of rift basins:
961 some implications thermo-isostasy, stress and rheology for intrabasinal structure, *Marine and*
962 *Petroleum Geology, 13,* 437-445.
963
964 Stephenson, R.A. and the EUROPROBE Intraplate Tectonics and Basin Dynamics Working
965 Groups (1993), Continental rift development in Precambrian and Phanerozoic Europe:
966 EUROPROBE and the Dnieper-Donets rift and Polish Trough basins, *Sedimentary Geology,*
967 *86,* 159-175.
968
969 Stephenson, R., Egholm, D.L., Nielsen, S.B., and Stovba, S.M. (2009), Thermal refraction
970 facilitates 'cold' intra-plate deformation: The Donbas foldbelt (Ukraine), *Nature Geosciences,*
971 *2,* 290-293.
972
973 Stephenson, R., Schiffer, C., Peace, A., Nielsen, S.B. and Jess, S. (2020), Late Cretaceous-
974 Cenozoic basin inversion and palaeostress fields in the North Atlantic-western Alpine-Tethys
975 realm: implications for intraplate tectonics, *Earth-Science Reviews, 210,* 103252.
976 doi:10.1016/j.earscirev.2020.103252
977
978 Stephenson, R.A., Yegorova, T., Brunet, M-F., Stovba, S., Wilson, M., Starostenko, V.,
979 Saintot, A. and Kusznir, N. (2006), Late Palaeozoic intra- and pericratonic basins on the East
980 European Craton and its margins, in *European Lithosphere Dynamics,* edited by D.G. Gee
981 and R.A. Stephenson, pp. 463-479, Geological Society of London, Memoir 32.
982
983 Stovba, S.M and Stephenson, R.A. (1999), The Donbas Foldbelt: its relationships with the
984 uninverted Donets segment of the Dniepr-Donets Basin, Ukraine, *Tectonophysics, 313,* 59-83.
985
986 Stovba, S.M. and Stephenson, R.A. (2003), Style and timing of salt tectonics in the Dniepr-
987 Donets Basin (Ukraine): implications for triggering and driving mechanisms of salt
988 movement in sedimentary basins, *Marine and Petroleum Geology, 19,* 1160-1189.
989
990 Stovba, S.M, Stephenson R.A. and Kivshik, M. (1996), Structural features and evolution of
991 the Dniepr-Donets Basin, Ukraine, from regional seismic reflection profiles, *Tectonophysics,*
992 *268,* 127-147.
993
994 Stovba, S.M., Tolkunov, A.P. and Stephenson, R.A. (2005), Regional investigations of
995 geological structure and evolution of the Donbas Foldbelt (DOBRE international project),
996 *Problems of the Petroleum and Natural Gas Industry, 1,* 21-34 (in Ukrainian).
997
998 Thomas, M.D. and Tanner, J.G. (1975), Cryptic suture in the eastern Grenville Province,
999 *Nature, 256,* 392-394.
1000
1001 Turcotte, D.L. and Schubert, G. (2002), *Geodynamics*, 2nd ed. Cambridge University Press,
1002 456 p.
1003
1004 Uyeda, S. and Kanamori, H. (1979), Back-arc opening and the mode of subduction, *J.*
1005 *Geophys. Res., 84,* 1049-1061.
1006
1007 van Wees, J.D., Stephenson, R.A., Stovba, S.M. and Shimanovsky, V. (1996), Tectonic
1008 variation in the Dniepr-Donets Basin from automated modelling of backstripped subsidence
1009 curves, *Tectonophysics, 268,* 257-280.
1010

Wilson, M. and Lyashkevich, Z.M. (1996), Magmatism and the geodynamics of rifting of the Pripyat-Dnieper-Donets rift, East European Platform, *Tectonophysics, 268*, 65-81.

Yamasaki, T. and Stephenson, R. (2011), Back-arc rifting initiated with a hot and wet continental lithosphere, *Earth and Planetary Sciences Letters, 302,* 172-184. doi:10.1016/j.epsl.2010.12.009

Yegorova, T.P. and Kozlenko, V.G. (2003), Refining the density model of sedimentary succession of south-eastern part of the Dnieper-Donets Basin and western part of the Donbas, *Geophysical Journal, 25*, 139-153 (in Russian).

Yegorova, T.P., Kozlenko, V.G., Pavlenkova, N.J. and Starostenko, V.I. (1995), 3-D density model for the lithosphere of Europe: construction method and preliminary results, *Geophysical Journal International, 121*, 873-892.

Yegorova, T.P., Stephenson, R.A., Kozlenko, V.G., Starostenko, V.I. and Legostaeva, O.V. (1999), 3-D gravity analysis of the Dnieper-Donets Basin and Donbas Foldbelt, Ukraine, *Tectonophysics, 313*, 41-58.

Yegorova, T., Starostenko, V., Kozlenko, V.G. and Yliniemi, J. (2004a), Lithosphere structure of the Ukrainian Shield and Pripyat Trough in the region of Eurobridge'97 region (Ukraine and Belarus) from gravity modelling, *Tectonophysics, 381,* 29-59.

Yegorova, T.P., Stephenson, R.A., Kostyuchenko, S.L., Baranova, E.P., Starostenko, V.I and Popolitov, K.E. (2004b), Structure of the lithosphere below the southern margin of the East European Craton (Ukraine and Russia) from gravity and seismic data, *Tectonophysics, 381*, 81-100.

Zaritskii, A.L. (1992), *Set of Maps, Geology and Metallogeny of the South-Western Part of the East-European Platform: Ukrainian Shield, Voronezh and Belarussian massifs, scale 1:1.000.000,* Geological Committee of Ukraine, Kyiv.

Ziegler, P.A. (1990), Geological Atlas of Western and Central Europe, 2nd ed. Shell Internationale Petroleum Mij. B.V. and Geological Society of London Publishing House, Bath, England, pp. 239.

Zonenshain, L.P., Kuzmin, M.I., Natapov, L.M. and Page, B.M. (1990), East European Platform, in *Geology of the USSR: A Plate-Tectonic Synthesis*, 3-16, AGU Geodynamics Series, 21.

1051 **Table 1.** Measured densities and P-wave velocities for the main rock types of the Ukrainian
1052 Shield (UkS) and Voronezh Massif (VM) from Krasovsky (1981) and Lebedev et al. (1986).
1053 Mean values are boldface and measurement ranges are in parentheses (where reported).
1054

Nominal crustal layer	Occurrence	Main rock types	Density ρ, Mg/m^3, (at atmospheric pressure)	P-wave velocity V_p, km/s (at the given pressure, p)	
				p=0.1 GPa	p=0.5 GPa
Upper layer (granitic-gneiss)	UkS	rapakivi granites	**2.66** (2.65-2.70)	**6.37** (6.28-6.46)	
	UkS	granites	**2.65** (2.60-2.70)	(5.9-6.25)	**5.28** (6.14-6.50)
	VM	granites	**2.67** (2.61-2.75)	**6.23**	**6.43** (5.75-7.26)
	UkS	migmatites	**2.64** (2.60-2.73)	**6.03** (6.0-6.3)	
	UkS	plagiogranites	**2.70** (2.68-2.72)	**6.12** (6.03-6.21)	
	VM	metasedimentary rocks	**2.74**		**6.05**
	VM	tuffs	**2.71** (2.64-2.78)		**6.20** (5.80-6.60)
	UkS	biotite-plagioclase gneisses	**2.73** (2.65-2.77)	**6.18** (5.88-6.25)	
	VM	shales	**2.82** (2.74-3.22)		**6.18** (5.90-6.60)
	UkS, VM	granodiorites	**2.71** (2.69-2.72)	**6.19** (6.11-6.27)	
	UkS	granosyenites	**2.685**	**6.19**	
	UkS	monzonites	**2.68**	**6.37**	
	UkS	Berdichev granites (ortite-bearing)	**2.74**	**6.25**	**6.40**
Middle layer (dioritic)	UkS	charnockites	**2.76**	**6.23**	**6.47**
	UkS	enderbites	**2.76**		**6.43**
	UkS, VM	diorites	**2.76**	**6.28**	
	UkS	rocks of intermediate composition	**2.75** (2.67-2.85)		**6.42** (6.22-6.50)
Lower layer (granulite-basaltic)	VM	mafic rocks	**2.94** (2.74-2.85)		**7.15** (5.84-7.60)
	UkS	mafic rocks	**2.84** (2.74-2.98(		**6.79** (6.33-7.10)
	UkS	anorthosites	**2.79**	**6.85** (6.82-6.92)	**6.99**
	UkS	gabbro-norites	**2.96**	**6.95** (6.85-7.05)	**7.02**
	VM	amphibolites	**2.90** (2.75-2.92)		**6.98** (6.95-7.10)
	UkS	pyroxene-plagioclase gneisses, pyroxene gneisses	**3.06** (3.05-3.09)	**6.82** (6.69-6.95)	

1055
1056

Table 2. Densities and velocities of DF (meta-)sedimentary rocks from Golizdra and Popovich (1999).

Stratigraphic unit	V_p (km/s)	ρ (Mg/m^3)
Lower Triassic (northern border zone)	≤ 3.0	2.1 (2.0-2.2)
Upper Carboniferous (northern border zone)	≤ 5.0	2.3
Upper Carboniferous	5.1-5.2	2.67
Lower Carboniferous Serpukhovian	5.3-5.4	2.68
Lower Carboniferous Tournaisian-Visean	5.6-5.7	2.70
Upper Devonian	5.7-5.8	2.71-2.72 (up to 2.8)

Figure captions

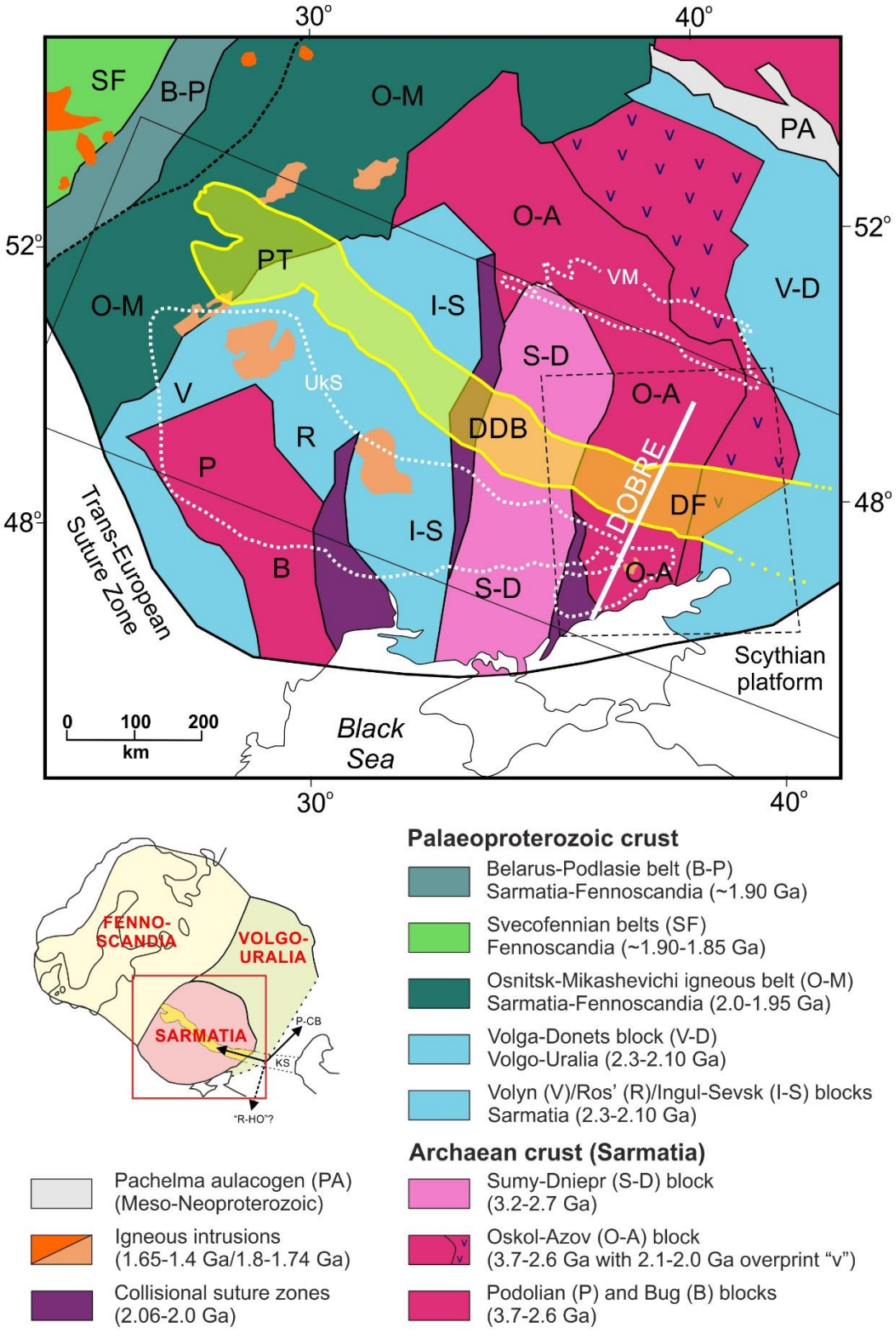

Figure 1

Figure 1. *Main map:* location of the Dniepr-Donets Basin (DDB) rift (yellow lens), including the northwestern Pripyat Trough (PT) segment and the southeastern inverted Donbas Foldbelt

(DF) segment over the regional basement geology of the Sarmatian segment of the East European Craton, modified from Bogdanova et al. (2008, 2016), Khain and Leonov (1996) and Gee and Stephenson (2006). Other abbreviated labels refer to basement units as identified in full in the figure legend. The thick, black dashed line represents the Sarmatian-Fennoscandian suture, with rocks of the O-M igneous belt northwest of it having a Fennoscandian tectonic overprint. The DOBRE profile discussed in the text is the labelled solid white line. The dotted white lines represent the approximate limits of the exposed crystalline basement of the Ukrainian Shield (UkS, south of the DDB) and the largely exposed part of the Voronezh Massif (VM, north of the DDB). The dashed black quadrangle corresponds approximately to the area of basement geology map in Figure 2. The incomplete black rectangle corresponds approximately to the area of the regional anomaly map in Figure 3a. *Inset regional map:* Sarmatia in the context of the Fennoscandian and Volgo-Uralian segments of the East European Craton, as defined by Bogdanova (1993) and Gorbatschev and Bogdanova (1993), as well as the location of the main map (red box). The three arrows on the inset map indicate a triple-rift system, such as postulated by Zonenshain et al. (1990), comprising the Late Palaeozoic DDB rift, the Peri-Caspian Basin (P-CB) rift and a since overprinted southerly-southwesterly rift that may have linked into the Variscan Rheno-Hercynian Ocean (R-HO) rift (e.g., Stampfli and Kozur, 2006), as discussed in section 6.2; KS is the Karpinsky Swell mentioned in section 2.2.

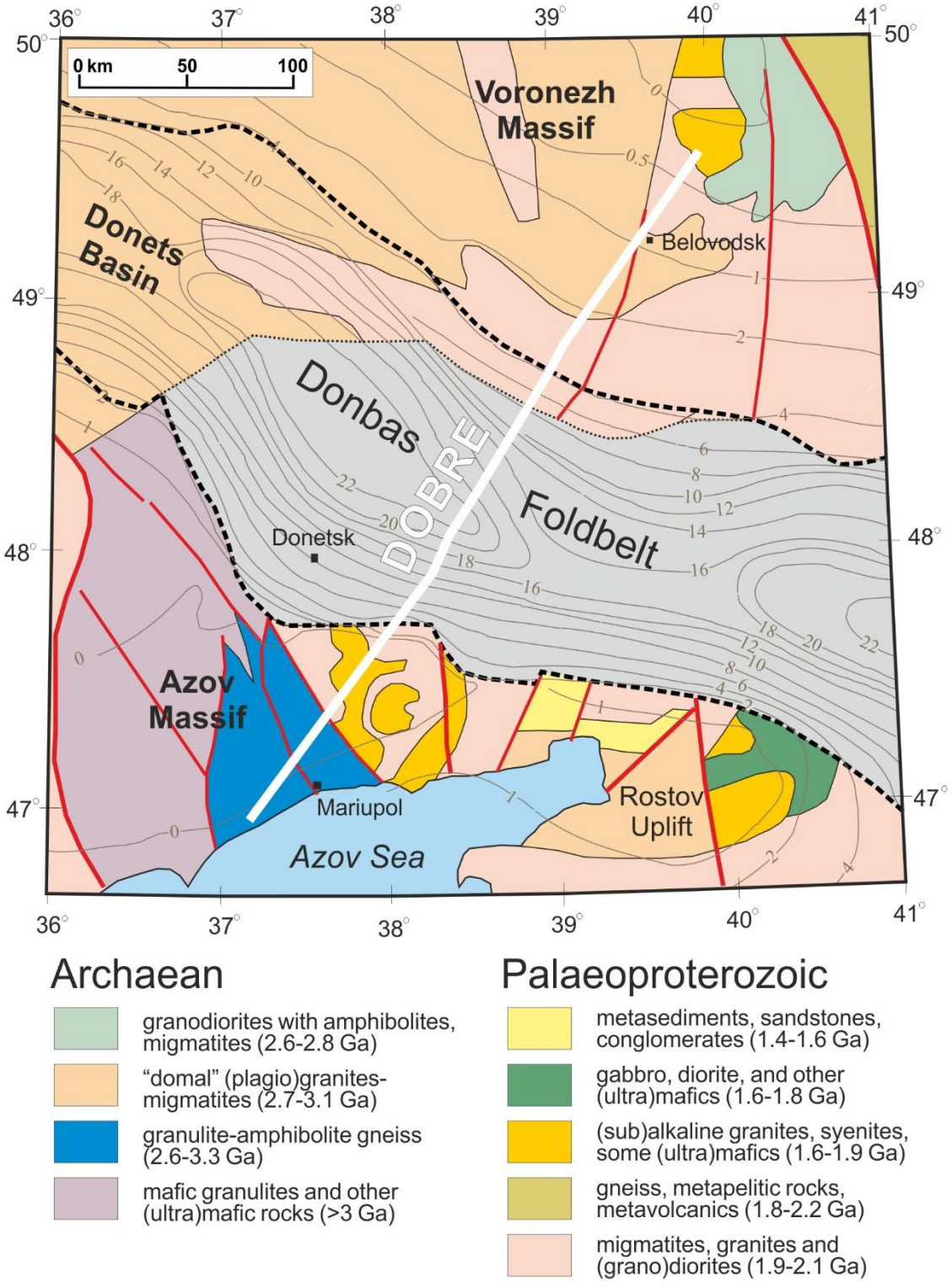

Figure 2

Figure 2. Basement geology of the study area (simplified from Zaritskii, 1992). The black dashed lines indicate this author's interpretation of the surface traces of the main rift-bounding faults of the DDB, including the DF. Grey colouring in the DF segment of the basin indicates that the basement geology is unknown (not penetrated by boreholes). Red lines are

(mostly inferred) basement faults. Depth-to-basement (base of Phanerozoic sedimentary cover) contours (km labels) are light grey, indicating exposed crystalline crust (< 0 km) within much of the Azov Massif, which is a prolongation of the Ukrainian Shield (cf. Fig. 1), and in the northeastern part of the Voronezh Massif covered by the map. The location of the composite seismic-gravity DOBRE profile (360 km long) is the white line. Map area is indicated in Figures 1 and 3.

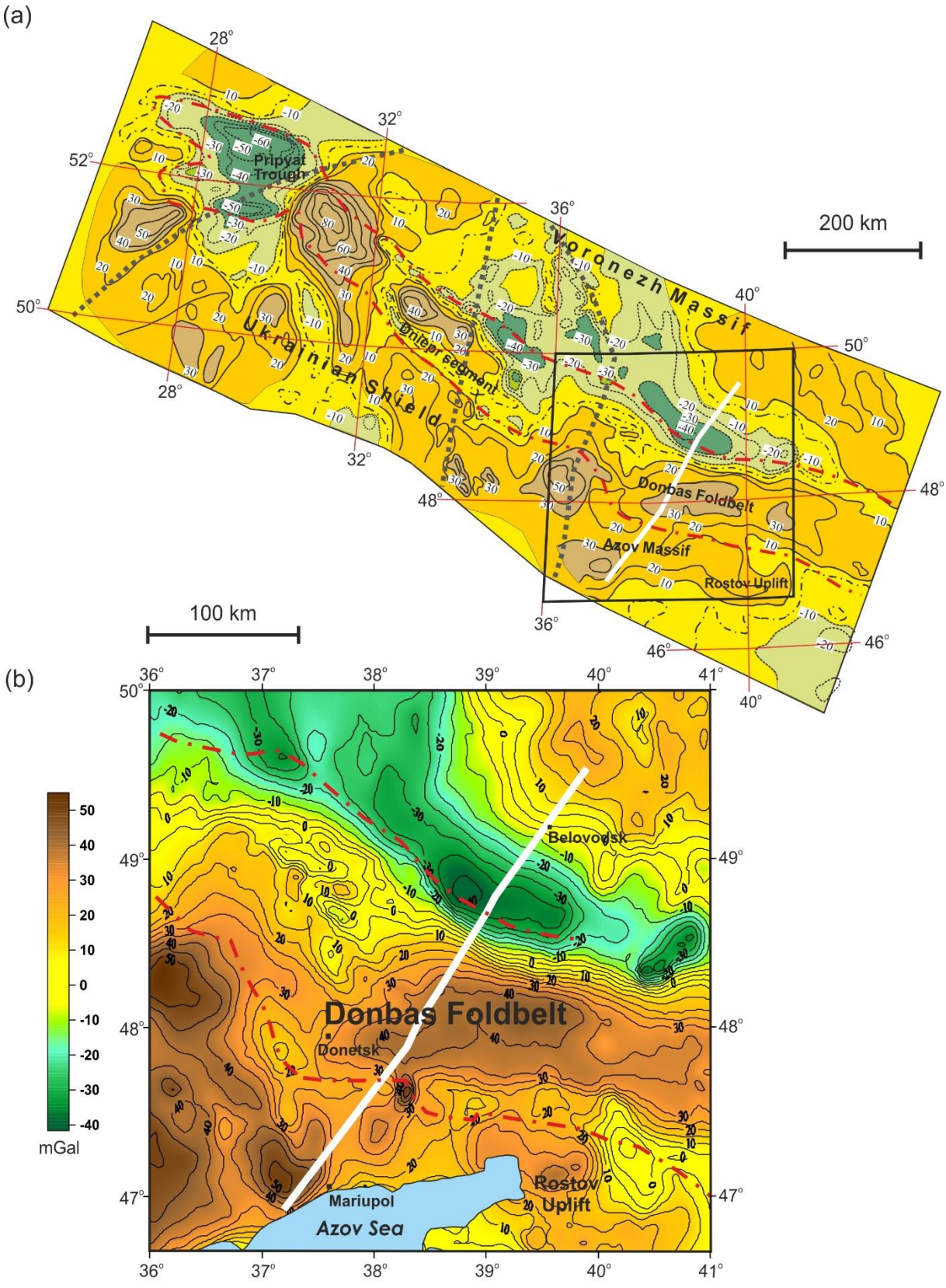

1099 Figure 3

1100 **Figure 3.** Bouguer gravity map (a) for the whole Pripyat Trough-DBB-DF (contour interval
1101 10 mGal), with the location of the DOBRE profile (white line) and showing the location of
1102 (b) a more detailed map (contour interval 5 mGal, every second line labelled) for the DOBRE

region (same area as Figure 2). The red dashed lines indicate the surface traces of the main rift-bounding faults of the Pripyat Trough-DBB-DF and the white lines indicate the location of the composite seismic-gravity DOBRE profile (360 km long) in both (a) and (b). The black dashed lines in (a) correspond to the traces of key basement boundaries indicated in Figure 1 (west to east): southeastern boundary of the Osnitsk-Mikashevichi igneous belt; boundary between the Ingul-Svesk and Sumy-Dniepr blocks; boundary between the Sumy-Dniepr and Oskol-Azov blocks. The gravity data are derived from the Ukrainian national database and have been gridded at an interval of 6 km from station values observed at an average spacing of 2 km Errors associated with the Bouguer anomalies are in the order of 1 mGal (cf. Nechayeva et al., 2002).

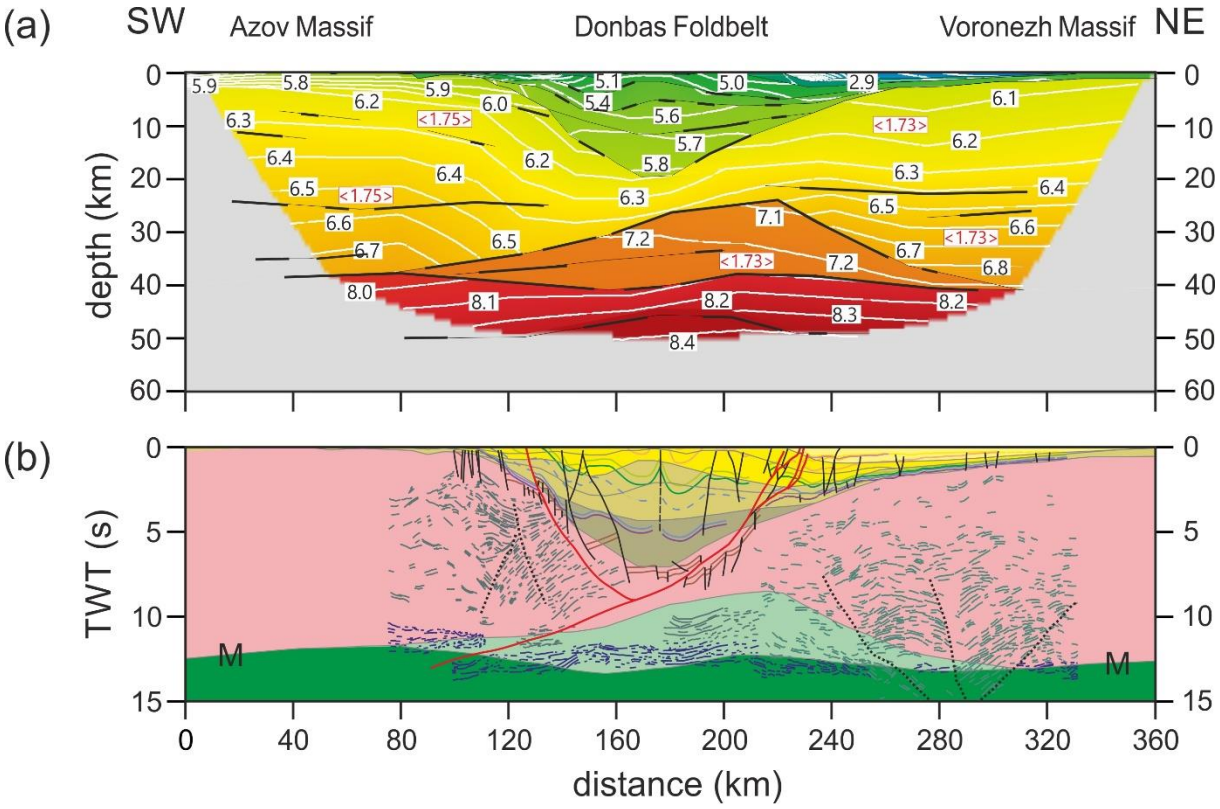

Figure 4

Figure 4. (a) Wide-angle reflection and refraction (WARR) velocity model along the DOBRE profile (DOBREfraction Working Group 2003) with P-wave velocity contours in km/s (colour bar: greens, < ~6.0-6.1 km/s supracrustal sedimentary succession; yellow-light orange ~6.1-6.8 km/s crystalline crust; dark orange, ~7.1-7.3 km/s, high-velocity lower crust; reds >8.0 km/s, upper mantle), V_p/V_s estimates red lettering with brackets; and with horizons producing wide-angle reflections shown with black lines. (b) Line drawing the DOBREflection 2000-2001 deep seismic reflection profile (Stovba et al. 2005, in large part based on the

interpretation of Maystrenko et al., 2003) superimposed on the WARR velocity model in part (a) converted to two-way travel time (TWT). Note that the low velocity uppermost sedimentary layers appear to be relatively much thicker in the TWT representation than in reality. Coloured layers in (b) pertain to the WARR model (see below); all other horizons (reflections and packages of reflections, including coherent horizons within the sedimentary succession) and (interpreted) faults refer to deep seismic reflection image. Non-inverted and inverted faults affecting the sedimentary body are black; the main faults involved in Late Cretaceous basin shortening, one cutting through the entire crust and an associated back-thrust, are indicated with slightly thickened red lines. WARR velocities in part (b) are as follows: sediments of the DF and its flanks (yellows to browns) lie in the range <3.0 km/s (on the northeastern flank of the basin, light green layer) to 5.8 km/s (for the deepest part of the DF, orange layer); crystalline crustal layer (pink) in the range 5.9-6.8 km/s; high-velocity lower crust (mint green) in the range 6.9-7.2 km/s; upper mantle (green) in the range 7.9-8.3 km/s. The Moho (labelled M), shown here with some velocity "pull-down", lies at a roughly uniform depth of 40 km.

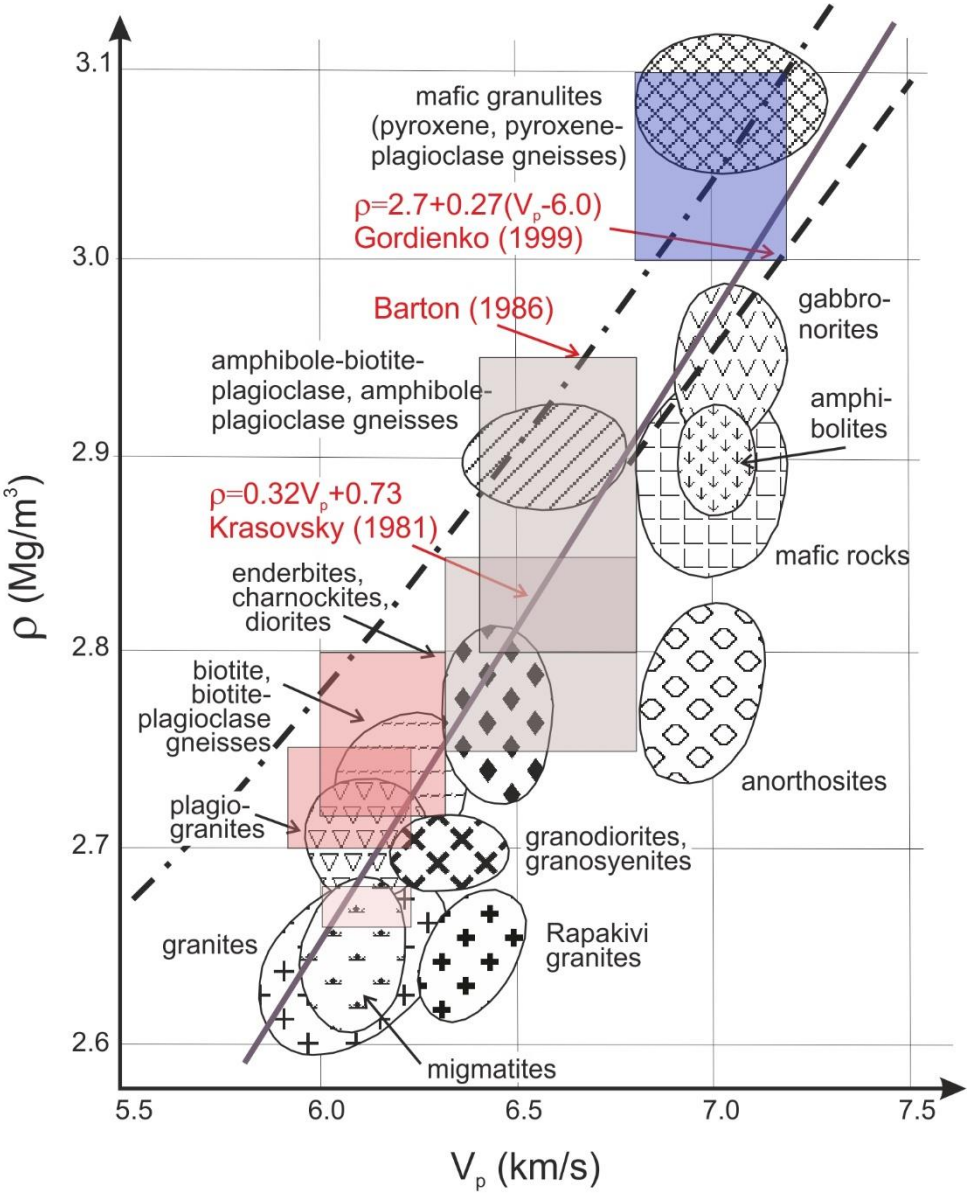

Figure 5

Figure 5. Graphical summary of observed velocity and density data for the major rock types in the Ukrainian Shield and Voronezh Massif (cf. Table 1). Shaded V_p-ρ domains are coloured according to crustal layers in the schematic compositional model seen in Figure 6b (pink upper crust, beige middle-lower crust, blue lower crust/rift pillow), with overlapping Voronezh Massif and Azov Massif domains lower-left and upper-right respectively. Straight lines are the V_p-ρ models mentioned in the text as labelled (red).

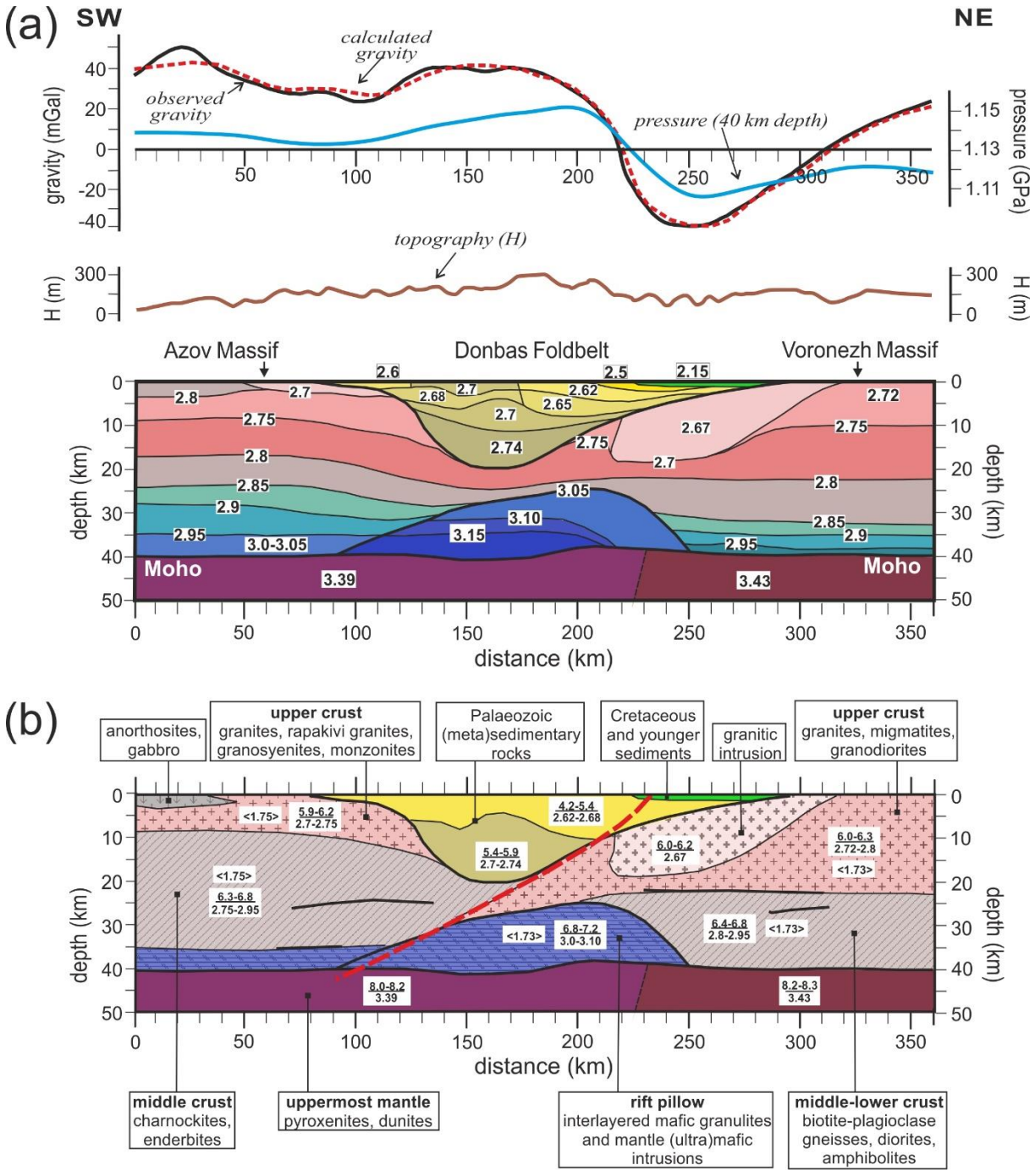

Figure 6

Figure 6. (a) Density model and (b) schematic compositional model with indicative rock-types along the DOBRE profile. Numbers in (a) indicate the model (bodies and layers) densities (in Mg/m^3) for the sedimentary successions of the DF and for the crust and upper mantle; the small arrows below "Azov Massif" and "Voronezh Massif" indicate the locations of the density profiles in Figure 7. Upper panels show gravity curves – observed (solid black line) and calculated (dashed red line) – and model pressure at the depth of 40 km (blue line) as well as topography (H; brown line) along the profile. Numbers in (b) indicate velocity

(km/s) and density (Mg/m^3) ranges, top and bottom respectively, as well as V_p/V_s ratio (in brackets). Thick solid lines show positions of wide-angle reflecting horizons (cf. Fig. 4, excluding sediment body) and red dashed line schematically indicates the position of master fault controlling Late Cretaceous inversion from Maystrenko et al. (2003). No kinematic implication is intended by the model geometry on either side of this fault, which has a throw of <5 km.

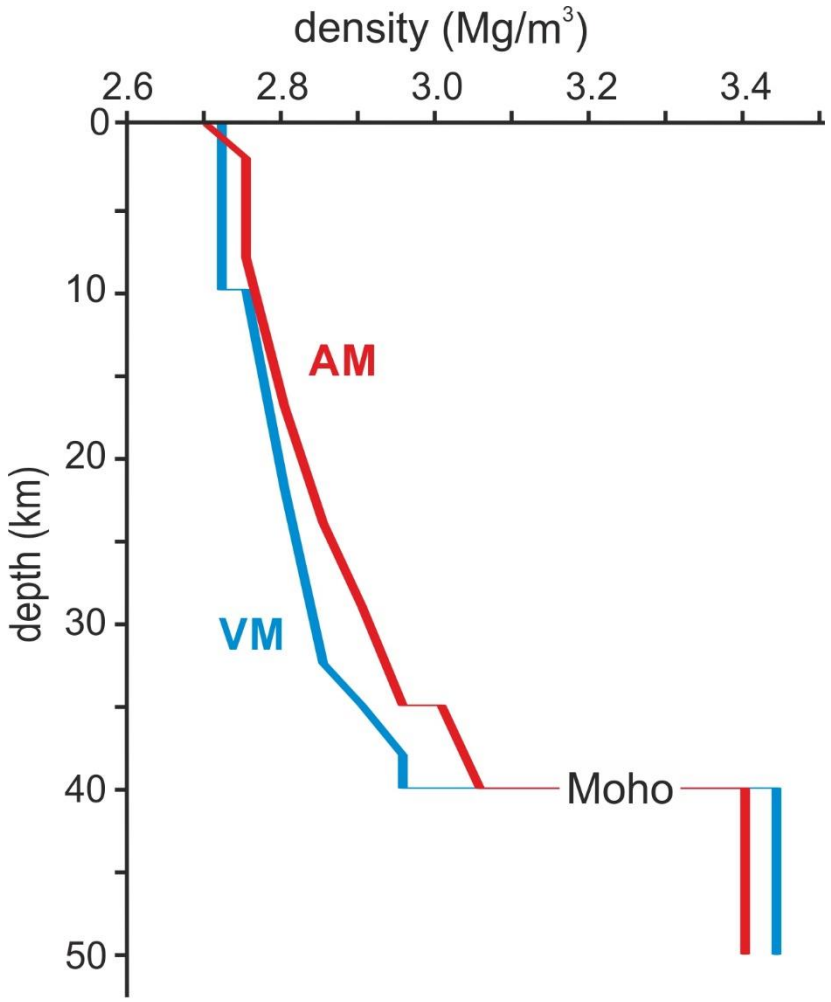

Figure 7

Figure 7. Density as a function of depth for the Azov Massif (AM) and Voronezh Massif (VM) contiguous to the Donbas Foldbelt from Figure 6a (precise locations indicated by respective vertical arrows).